POLITECNICO DI TORINO

Master program in Nanotechnologies for ICTs

Thesis of Master degree

October 2022 Graduation Session

Translating Aptamer-Modified Nanopipettes to Complex Systems

Supervisors

Dr. Nako NAKATSUKA

Prof. Matteo COCUZZA

Prof. Janos VOROS

Candidate

Anna Burdina

Academic Year 2021/2022

Summary

Dopamine is a type of neurotransmitter and hormone. It plays a role in many important body functions, including movement, memory, pleasurable reward and motivation. High or low levels of dopamine are associated with several mental health and neurological disorders. With these diseases being on the rise, it is imperative to improve understanding of the basics of neuronal transmission. Limitations in the selectivity and sensitivity hinder most biosensor platforms from detecting physiologically relevant changes in neurotransmitter concentrations real time. Moreover, spatial resolution nearing synaptic ranges 20-40 nanometers (nm) stays challenging for most of the state-of-the-art techniques.

Dopamine specific nanopipette sensor claim to be a promising candidate for serving these issues. The working mechanism of a nanopipette is a combination of ion rectification effect which allows to sense extremely small ion changes in buffer solution and/or sensor's surface charge alternations, and surface coating with specific molecules termed aptamers that provide selectivity.

This Master's Thesis focuses on the characterization of the dopamine specific nanopipette working principle. More precisely, the origin of the nanopipette current response was investigated by means of QCM-D and novel technique termed Focal Mology Graphy. Several hypotheses had been put forward in order to explain diverse sensor behavior in presence of divalent cations. In addition, dopamine nanopipette sensors were used for dopamine quantification in complex media such as blood serum and neuron culture media. Moreover, yield analysis was performed and the whole sensors functionalization process was reviewed. As a result yield increase of nearly 2 times was achieved.

Laboratory environment and Team

ETH Zurich is a public research university in the city of Zürich, Switzerland. It unites students, professors and researchers in all the engineering areas. ETH Zurich is accounted to be in the top 10 universities worldwide for their high scientific contribution.

Laboratory of Biosensors and Bioelectronics (LBB) is a part of Institute for Biomedical Engineering, Department of Information Technology and Electrical Engineering. The laboratory mainly focus on development of novel micro- and nanotechnology based sensing approaches for diagnostics and drug discovery in collaboration with industrial and academic partners, as well as on using nanobiotechnology in medical devices and for building, modeling and interfacing neural networks. The head of the laboratory and one of the principal investigators Prof. Dr. Janos Vörös.

Nako Nakatsuka, my supervisor, is a senior scientist and principal investigator of the LBB group. Her focus lies on understanding the fundamental molecular interactions of DNA-based recognition elements termed aptamers that capture small-molecule targets with high specificity and selectivity. Her team research trajectory includes elucidating and harnessing the mechanisms of aptamer-target interactions enabling the design and development of next-generation nanotools for diverse applications such as biosensing, clinical diagnostics, and drug discovery.

Acknowledgements

Foremost, I would like to express my sincere gratitude to my supervisor Dr. Nako Nakatsuka for the continuous support of my project and research, for her patience, motivation, enthusiasm, and immense knowledge. Moreover, I would like to thank my mentor, Ph.D. student, Annina Stuber. Her guidance helped me in all the time of research and writing of this report.

Besides my ETH advisors, I would like to thank: Matteo Cocuzza for guiding me throughout the research process, supporting and providing me with all the needed information; Julian Hengsteler for his availability, support, and his irreplaceable help with all the electronic devices and laboratory facilities; Andreea Aura Manole for providing us with clinical samples; Alessandra Arizzi, for her availability, support, guidance throughout the Lino Biotech measurements and, of course, for the provided chance to work with Lino setup.

My sincere thanks also go to Prof. Dr. Janos Vörös, without who this internship would not be possible.

Table of Contents

List of Tables

List of Figures

Chapter 1

Introduction

The understanding of brain function, which remains largely a mystery, is one of the grand scientific challenges of today. Neurons, the fundamental units of the brain and nervous system, perform information exchange through a combination of action potentials as well as the release and capture of small molecules termed neurotransmitters. Neurotransmitters, neuromodulators, and their interactions are involved in countless functions of the nervous system and controlling bodily functions. Thus, any concentration imbalance in the brain may lead to physical or mental dysfunction[1], [2]. The study allowing the understanding of the functionality and influence of neurotransmitters requires high sensitivity, specificity, and selectivity since the molecules are found in a complex environment. Further, interrogation of neuronal communication requires high spatial resolution, ideally nearing nanoscale synaptic ranges (20-50 nm), and temporal resolution on the order of milliseconds to track neurotransmitter release in real-time.

Dopamine, the target molecule of the present thesis work, is believed to be released during stimulus-to-action sequences such as reinforcement learning, decision-making, and motor control [3]. The dysfunction of dopamine target circuits has been linked to disorders such as Parkinson's disease, schizophrenia, and addiction [4], [5], [6]. Thus, the dopamine system has long been the focus of intense study and ongoing work continues to elucidate its role in controlling brain function and behavior.

This thesis is focused on the functionalized nanopipette sensor, which enables the detection of subnanomolar dopamine concentrations (physiologically-relevant range up to $\sim$ 10nM) ideally to be detected within the sub-second temporal resolution and spatial resolution of the order of tens on nanometers. The core mechanism of the pipette functionality lies in the surface coating with short, single-stranded DNA molecules called aptamers that can selectively bind to a specific target molecule.

1.1 State-of-the-art

To explain the need for the nanopipette sensor, state-of-the-art techniques for dopamine detection will be discussed. First, an introduction to the two methods which are considered the most mature and widely used for neurotransmitter detection is given: microdialysis and fast scan cyclic voltammetry (FSCV).

Microdialysis. Microdialysis uses a dialysis bag to collect samples from the brain. Small molecules diffuse across the semipermeable membrane ($\sim$ 200 µm outer diameter [7]) into the internal dialysate fluid of the dialysis probe. Once the cerebrospinal fluid is collected, its analysis and quantification can be performed by various techniques such as high-performance liquid chromatography [8], capillary electrophoresis [9], mass spectrometry [10], and electrochemistry [11]. Depending on the technique that is used and the sampling rate, microdialysis is capable of high sensitivity and selectivity, permitting quantification of low concentrations of multiple compounds from select brain regions [12].

Among the advantages of the microdialysis technique is the symmetrical probe, which generates an evenly affected area of the tissue. The microdialysis membrane serves as a physical barrier between the tissue and the perfusate. This separation protects the tissue from the turbulent flow of the perfusate and limits the penetration of high-molecular-weight substances. Moreover, microdialysis has been demonstrated to be sensitive to dopamine detection in vivo, with a limit of detection (LOD) as low as 5 pg/mL [13]. However, this method has several disadvantages when compared to the other sensing techniques. Yocky *et al.* [14] summarised the progress of the microdialysis approach for dopamine detection and highlighted the drawbacks of this method. Although microdialysis is highly sensitive and specific, temporal resolution is limited by the rate of sample retention and separation, meaning microdialysis samples do not provide real-time information regarding changes in the neurochemical environment because their typical collection rate is in the range of seconds to minutes(include ultrafast microdialysis). Secondly, the solutes capable of crossing the dialysis membrane can affect basal levels and/or the pharmacological responsiveness of the tissue under the study. The perfusion itself may induce changes in the surrounding brain tissue, which may influence the release and metabolism of the sampled transmitter. Third, the probe still causes damage to the tissue and drastically decreases the spatial resolution which is of paramount importance for neurological studies performed in cells. Fourth, the dialysis technique requires tissues deep enough for the probe to be inserted. This aspect limits the choice of the brain regions to be analyzed. Finally, the flow rate for collecting dialysate fluid is generally kept low to maintain high relative recovery and in an attempt to minimize tissue damage or alter diffusion pattern and so the quantity of analyte collected represents only a fraction of the actual extracellular

concentration. All these challenges led to the development of alternative monitoring approaches, one of them being FSCV.

FSCV. FSCV is an electrochemical technique that consists of repeatedly applying voltage waveforms to the electrode to detect time-dependent changes in current. These changes are proportional to the concentration of electroactive molecules at the electrode surface. The output curve shape and its peak positions are specific for each neurochemical and voltage amplitudes are designed to detect different electroactive molecules based on distinct reduction and oxidation potentials.

Compared to microdialysis, FSCV matches the time scale of neurotransmitter release and provides high temporal (x ms) and higher spatial resolution due to a smaller probe ($\sim$ tens of µm diameter [15]), which has made FSCV an instrumental technique for quantifying terminal neurotransmitter release mechanisms. Among the advantages, the carbon-based electrodes provide biocompatibility [16]. Another recent development involves miniaturized carbon fiber probes with a cross-sectional area that is >100 times smaller than conventional carbon fiber electrodes reaching a probe size of a few micrometers [17][18]. These 'micro-invasive' probes produce minimal tissue disruption and provide stable performance for over a year.

Yocky *et al.* [14] and Rafi *et al.* [19] analyzed the recent accomplishments and drawbacks of FSCV in dopamine detection. Recorded changes in current are proportional to dopamine concentration changes across a physiologically-relevant range (10 nM to 10 µM) and are detected on a subsecond timescale (10 Hz). However, due to the similarity of the oxidation potentials of different molecules, the selectivity in the complex matrices needs to be improved, thus FSCV is particularly challenging for differentiating dopamine vs. l-3,4-dihydroxyphenylalanine (L-DOPA) vs. norepinephrine. Another drawback is system fragility - the electrode loss due to breakage of the carbon fiber or its connection to the electrical equipment. Moreover, signal interference due to electrical noise or movement artefacts is a frequent concern, particularly in behaving animals.

Recent progress. Latest advances in electronics, nanotechnology, and biotechnology allows the existence of a wide range of solutions for neurotransmitter detection overcoming the limits of microdialysis and FSCV. Table 1 summarise several state-of-the-art sensing approaches based on electrochemical and optical signals, which apply to dopamine detection both *in vitro* and *in vivo*.

Optical techniques such as G-protein-coupled receptor-activation-based (GRAB) sensors take advantage of naturally occurring neurotransmitter receptors. These sensors convert a ligand-stabilized conformational change in the dopamine receptor into an optical response via a conformation-sensitive fluorescent protein inserted in the receptor's third intracellular loop. Moreover, GRAB sensors proved capable of detecting nM concentrations, which is in the physiological range for

most neurotransmitters detection, and providing high selectivity over non-target molecules [20]. The variety of fluorescent proteins enables several orthogonal readouts of distinct neurochemical events. Among the disadvantages, there is the inability to achieve a spatial resolution below the micrometer scale. Moreover, different fluorescent proteins have distinct fluorescent properties such as intensity, and signal duration, which could lead to variable signal intensities at different penetration depths.

The second optical technique frequently used to detect small molecules in complex media is the cell-based neurotransmitter fluorescent engineered reporters (CNiFERs) [21]. Similar to GRAB sensors, a CNiFER technology utilizes the clone of the native receptor for a particular neurotransmitter, e.g., D2R for dopamine. Advantages of this method include nM limit of detection and temporal response in the order of seconds. Among the disadvantages of this approach is the procedure of the cell insertion into the tissue of interest, which may lead to inflammation. Micrometer spatial resolution still limits experiments on the cell level and due to the degradation of the fluorescent proteins, sensing inside the same tissue cannot be performed over a long time, and thus long-term activity can not be monitored. To this end, optical techniques are sensitive enough to detect neurotransmitters such as dopamine, but both GRAB and CNiFER sensors lack spatial resolution for measurements near synapses.

Aptamers based sensing An alternative approach involves aptamer-based sensing techniques. Aptamers are oligonucleotide or peptide molecules that bind to a specific target molecule that rivals those of monoclonal antibodies. The story of the aptamer's discovery dates to 1990 when the greater research community began to consider the selective binding potential of DNA and RNA and the advantages of oligonucleotides as affinity agents [22].

Since then, aptamers research has been expanding, bringing the ability to detect increasing numbers of targets including proteins, peptides, carbohydrates, small molecules, viruses, ions, toxins, and even live cells [23]. The advantages of aptamers include high specificity, small production cost, prolonged storage life, minimal batch-to-batch differences, facilitating the detection of electrochemically inactive compounds, low immunogenicity, and feasibility of chemical modifications for enhancing stability compared to monoclonal antibodies [23].

One of the working mechanisms of the aptamers lies in the conformational change of the DNA backbone structure, thus leading to a significant modification in the aptamer's occupied area and a change in the charge distribution on the surface where the analyte is present. This core principle of aptamers makes them a perfect candidate for the combination with the variety of sensor setups [24], [25], [26].

Several research groups investigated the performance of the dopamine-specific aptamer through a transistor-based technique. Aptamers are functionalized on the surface of the semiconducting surface of the transistor, thus the target-induced reorientation of the negatively charged aptamer backbones in close proximity to the thin films modulates the charge distribution resulting in a measurable change in current. Nakatsuka *et al.* [27] detected t sub-pM concentrations of dopamine in phosphate-buffered saline (PBS) and artificial cerebrospinal fluid (aCSF) and proved high specificity of the sensor compared to similarly structured molecules such as norepinephrine, L-DOPA, and 3,4-dihydroxyphenylacetic acid (DOPAC). Later, Wu *et al.* [28] employed a different micro transistor technology but used the same DNA aptamer to monitor dopamine release in vivo. The team achieved physiologically relevant temporal resolution and high specificity, although the probe size of around a hundred micrometers still limits the spatial resolution rendering mapping of synaptic dynamics impossible.

The need for sensitive and selective dopamine-specific sensors having the spatial resolution on the order of nanometers gave rise to the development of the aptamer-modified nanopipette. Moreover, nanopipettes are advantageous in their ease of fabrication, low cost, and miniature size. The applicability of the nanopipette technique for neurotransmitter detection was previously demonstrated by Nakatsuka *et al.* [29]. The team demonstrated high specificity, selectivity, and sensitivity for in vitro detection of 5-hydroxytryptamine also called serotonin (5-HT) in complex media using serotonin-specific DNA aptamer-functionalized nanopipettes (tip diameter 10 nm). The real-time current measurement inside the neurobasal medium (NBM) demonstrated selectivity versus similarly structured molecules L-5-hydroxytryptophan (L-5-HTP) and 5-hydroxyindoleacetic acid (5-HIAA). Since biological and pharmaceutical sensing often requires long-term measurements and stability, serotonin sensor measurements were conducted for at least 4 h without clogging in NBM with minimal changes in performance.

To this end, nanopipette embedded with target-specific aptamers appear to be promising for real-time dopamine detection at subnanomolar concentrations and can conduct minimally invasive experiments. The next chapters will cover the fabrication and the detection mechanism of dopamine-specific nanopipette sensors.

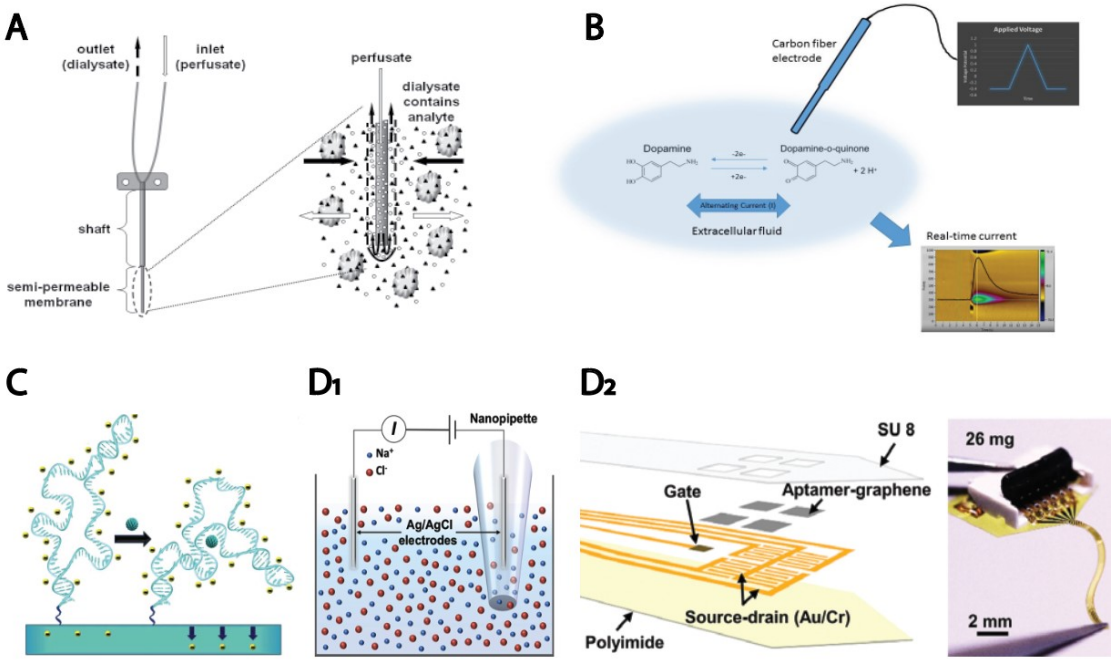

Figure 1.1: State-of-the-art probe-based techniques for neurotransmitter detection. **(A)** The microdialysis probe is designed to mimic a blood capillary and consists of a shaft with a semipermeable hollow fiber membrane at its tip, which is connected to inlet and outlet tubing. The probe is continuously perfused with an aqueous solution (perfusate) that closely resembles the ionic composition of the surrounding tissue fluid. Once inserted into the tissue or fluid of interest, small solutes can cross the semipermeable membrane by passive diffusion. When the solution of interest is collected it is analyzed by various techniques such as capillary electrophoresis, electrochemistry, mass spectrometry and high-performance liquid chromatography. Adapted from `https://en.wikipedia.org/wiki/Microdialysis` **(B)** FSCV utilize a carbon fiber electrode to quickly change the voltage to oxidize the molecule of interest (dopamine). The resulting alternating current is used to find the instantaneous concentration of dopamine in the extracellular fluid by analyzing current peak width and position. Adapted from `https://en.wikipedia.org/wiki/Fast-scan_cyclic_voltammetry`. **(C)** Aptamers deposited on the probe surface undergo hypothesized mechanism of stem-loop aptamer target-induced reorientations in close proximity to charged surface and within or near the Debye length. Aptamers reorient closer to the surface thus depleting channels electrostatically. Adapted from [27]. **(D)** Possible setups to implement aptamer surface coating as a part of recognition mechanism. (D_1) Nanopipete coated with aptamers on the inner surface measures ionic flux through the pore when inserted into solution of interest. Upon binding to target molecule, aptamers backbone reorientation causes alteration of surface charge, thus modifying the strength of ionic flow. Adapted from [29]. (D_2) Field Effect Transistor based probe coated with aptamers layers able to modify the conductivity of the semiconductor gate level upon recognition. Upon target identification aptamers cause depletion of charged particles, modifying channel length of the transistor. Adapted from [28].

Setup	Imaging approach	Reaction time	LOD	Mediums tested	Specificity (+ no signal / - signal comparable to the target molecule)	Analysis was performed in vivo / in vitro	Source
FSCV	electrochemical	s	9 nM	Tris Buffer	- L-DOPA - norepinephrine	In vitro	Kelmendi B. *et al.* [30]
GPCR activation based (GRAB) sensors	optical	s	4 nM	+ HEK293T + rat cortical neurons + transgenic flies	+ 1 µM haloperidol + dopamine + 1 µM eticlopride + 1 µM serotonin + 1 µM glutamate + 1 µM Gamma-aminobutyric acid (GABA) + 1 µM adenosine + 1 µM acetylcholine + 1 µM tyramine + 1 µM octopamine + 1 µM L-DOPA - 1 µM SCH + dopamine	both	Fangmiao Sun *et al.* [20]
GPCR activation based CNiFERs sensor	optical	s	2.5 ± 0.1 nM	+ HEK293 cells + ventral striatum (nucleus accumbens) and medial prefrontal cortex + substantia nigra (SN) DA neurons	+ 1 µM Orexin + 1 µM Glutamate + 1 µM GABA + 1 µM Acetylcholine + 1 µM VIP + 1 µM Histamine + 1 µM Substance P + 1 µM Adenosine + 1 µM Melatonin + 1 µM Serotonin - 1 µM Somatostatin	in vitro	Arnaud Muller *et al.* [21]
Aptamer–field-effect transistors	electrochemical	s	1 pM	+ PBS + aCSF	+ 100uM Serotonin + 100uM norepinephrine + 100uM L-DOPA + 100uM 3,4-dihydroxyphenylacetic acid (DOPAC)	In vitro	Nako Nakatsuka *et al.* [27], [31]
Aptamer-Graphene Microtransistors	electrichemical	ms	10 pM	+ aCSF + (dorsal striatum ex vivo and in vivo, however no LOD analysis was performed)	+ 100 µM Serotonin + 100 µM Norepinephrine + 100 µM GABA	both	Guangfu Wu *et al.* [28]
Graphene Aptasensor Multitransistor Arrays	electrichemical	ms	1 aM	+ PBS + aCSF + CSF rat dopamine - depleted brain regions	+ 1 nM L-DOPA + 1nM L-tyrosine + 1 nM ascorbic acid in 1 × PBS	both	Mafalda Abrantes *et al.* [32]

Table 1.1: Comparison between several state-of-the-art techniques for dopamine sensing.

Chapter 2

Aptamer functionalized nanopipette sensor for dopamine detection

2.1 Ion Current Rectification

Systems based on nanopores enable insights into chemical and electrical events within micro- or nanoscale due to the confined sensing space [33], [34]. In recent years nanopores in the form of quartz micro- and nanopipettes have attracted attention due to the ease and low cost of fabrication, variety of surface coating, and facility of use [35]. A phenomenon observed with nanopipettes and many other nanopores is ion current rectification (ICR), which describes the asymmetric i–V relationship for ion transport (see figure 2.1). ICR has been extensively studied over the last years. Predominant models [36] suggest that the origin of this effect lies in the depletion or accumulation of counter ions at the charged surface of the nanopipette tip which results in asymmetric ionic flux through the opening when a negative or positive bias is applied. The alternation of counter ions on the quartz surface influences the conductivity through the pore in a nonlinear manner.

In order to be able to quantify and analyze ICR effect within nanopores and its dependency on the environmental factors several approximations were established [37], [38], [39]. One model suggests that total ionic flux constitutes three components [40]: the diffusive, electro-osmotic, and convective flux which are integrated across the whole area of the nanopipette tip. The resulting current is the total ionic current through the nanopipette orifice. The ionic simplified model of current I

through the nanopore can be evaluated [41]:

$$I = \int_{\Omega} F(\sum_{j}^{2} v_j N_j) n \, d\Omega$$

where the first, and second terms of N_j are the ionic flux due to the convection, and diffusion, respectively, v_j is the valence of the jth ionic species, n is the unit outer normal vector of the corresponding surface, Ω is the surface of the reservoir end.

To the date [42], [43], [44], [45], [46] the ICR phenomena and its characteristics are investigated in terms of the governing parameters such as salt type [45], the bulk ionic concentration Co [47], [42], [43], [45], [48], pH of the electrolyte [49], and the surface charge density σ [44], [50]. It is reported that the ICR phenomena accentuate the increasing value of pH, σ, Co, and the electronegativity of the salt cation. Moreover, the density of the bulk solution affects the ionic flow through the nanopipette in an inverse manner [40].

Nanopipette used for dopamine detection has aperture size in the order of ten's nanometers. The tiny pore, as well as the tip angle, allows sensing up to ten's of pA current changes which are the result of charge distribution change on the capillary surface and/or difference in the ionic content in the buffer solution.

2.2 Dopamine specific aptamer

To ensure the selectivity of the dopamine nanopipette the surface is coated with dopamine-specific aptamers. Similar to serotonin aptamers [29] dopamine aptamers undergo conformational change upon binding with the target [27]. The backbone reorientation causes the alternation of charges on the pipette interior, thus modifying the conductivity (see figure 2.2 B).

Observations and previously conducted experiments with the same dopamine specific aptamers suggest a current decrease upon target recognition [28], [27]. Obtained during this Master's Thesis results constitute to not straightforward behavior of the aptamers. The majority of the experiments led to low conductivity upon binding (see figure 2.3), however, change of ionic content inside the solution of interest brought an increase of conductivity. The origins of these changes were studied and handed out in the result section.

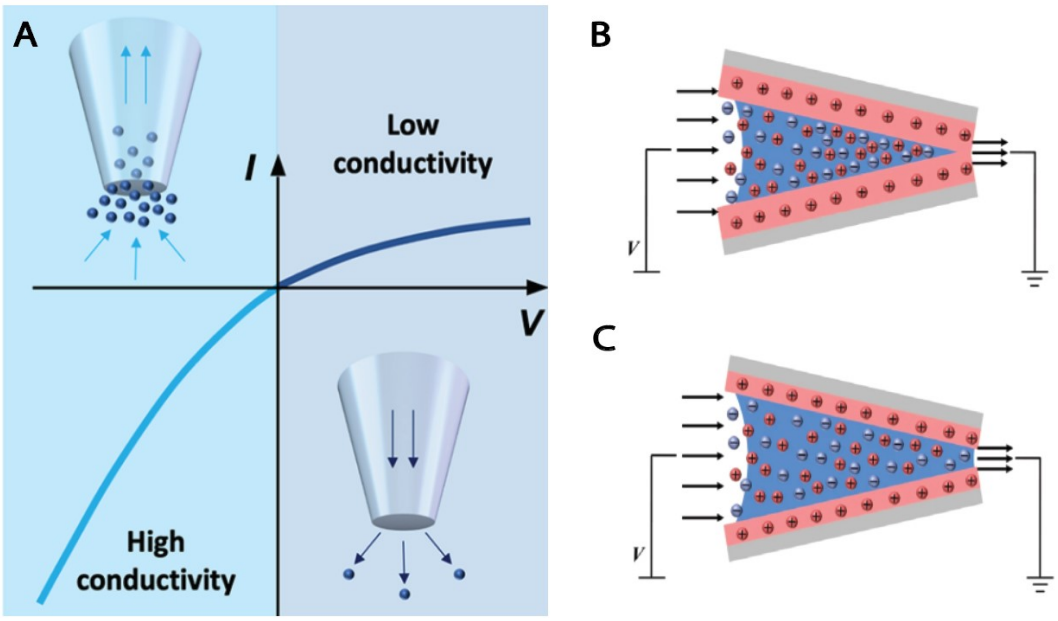

Figure 2.1: Ion Current Rectification. **(A)** ICR introduces asymmetric flux of ions through the nanopore whereby nanopipettes respond to a symmetrically applied voltage sweep with a nonlinear asymmetric current output, deviating from ohmic behavior. Adapted from [29]. **(B)** Conical nanopore with a forward potential bias. The electric double layer is highlighted with red shading. The blue shading represents the bulk solution. When electric double layers are thick and interaction occurs at the nanopore tip. **(C)** When they are thin and there is no interaction. Dimensions are not to scale. Adapted from [40].

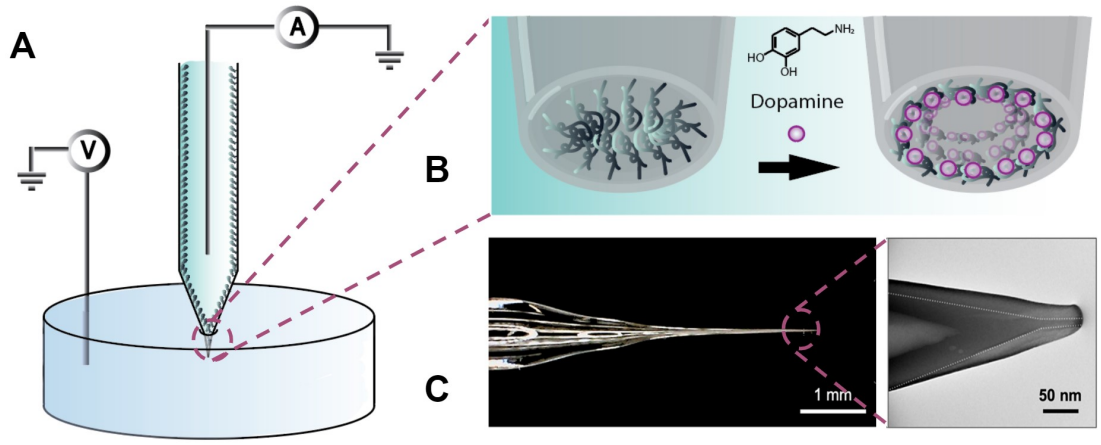

Figure 2.2: Nanopipette working principle. Possible nanopipette measurement setup **(A)**. Aptamers undergo a structural switch upon dopamine biding **(B)**. Scanning electron Microscopy images adapted from [29] zoom tip orifice of about 10 nm in diameter **(C)**.

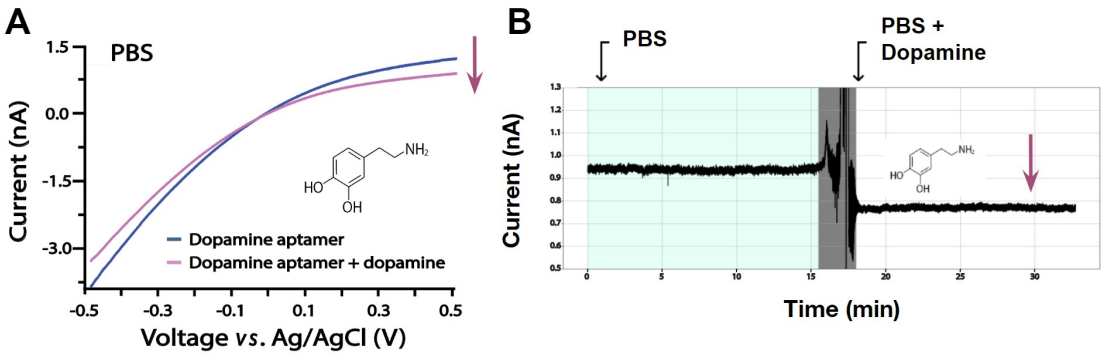

Figure 2.3: The current magnitude decrease upon binding with dopamine is distinguishable both during CV **(A)** and real-time **(B)** measurements.

Chapter 3

Experimental Methods and Techniques

3.1 Materials

All chemicals if not otherwise stated below were provided by SigmaAldrich Chemie GmbH (Buchs, Switzerland). For all measurements, the phosphate buffer saline (PBS) at pH 7.4 and at 1x concentration (see table 4.1) (ThermoFisher Scientific AG, Reinach, Switzerland) was used as received. For several chemical deionized water with resistivity 18.2 $M\Omega cm^{-1}$ produced by a Milli-Q system (Millipore, Billerica, MA) was used. Thiolated single-stranded dopamine aptamer: (5'/Thiol/CGA CGC CAG TTT GAA GGT TCG TTC GCA GGT GTG GAG TGA CGT CG 3') with molecular weight 13,969.8 g/mol, melting point 74 $°C$ .To have a significant difference in the secondary structure versus the target-specific sequence, the scrambled sequence was designed by modelling via MFold. Thiolated scrambled sequence: (5'/Thiol/AGT ACG TCG ATG CTC GAT CAG TGG GCT AGG TGC GTA GCG GTC TG 3') with molecular weight 13.8718 g/mol, melting point 73.7 $°C$, were purchased from Microsynth AG (Balgach, Switzerland). Until usage all DNA solutions (100 µM) were aliquoted, HPLC purified, and stored at -20 $°C$.

3.2 Methods

Nanopipette Fabrication: Quartz capillaries (o.d., 1 mm; i.d., 0.5 mm; Friedrich Dimmock) are fixed at the edges and pulled apart(P2000, Sutter Instruments), while the laser beam heats the middle. The pulling parameters for the nanopipettes with apertures 10 nm ± 5 nm (see figure 2.2 B): (line 1) Heat 750, Filament 4, Velocity 40, Delay 150, and Pull 80; (line 2) Heat 700, Filament 3, Velocity 60,

Delay 135, Pull 180. The laser puller was preheated for at least 1 h before use.

Figure 3.1: CVD custom setup. The nanopipette holder consists of a glass flusk with streatchable cup covering nanopipette holder. Pipettes are fixed vertically and a cup containing fresh saline is posed at the bottom of the holder. The system is then brought under vacuum and inserted into a constant temperature bath for 1 hour. Picture is adapted from A. Failletaz Master's Thesis [51].

Aptamer functionalization: DNA aptamers are immobilized on the inner surface of the nanopipette via a three-step procedure. First, (3-aminopropyl)-trimethoxysilane (APTMS) was deposited on the nanopipette surface by Chemical Vapour Deposition (CVD). Pulled pipettes are inserted into a vertical holder (see figure 3.1). The nanopipette holder is then inserted into a flask containig approximately 500 µL of fresh saline in a cup. The vacuum was created by soaking the air during 2 min. and the system rest for 1 h. at 40 °C. Second, pipettes were filled with 1 mM solutions of 3- maleimidobenzoic acid N-hydroxysuccinimide ester (MBS) dissolved in a 1:9 (v/v) mixture of dimethyl sulfoxide and PBS. The solution was left over for one hour. DNA aptamers of concentration 100 µM previously incubated with 50-fold excess tris(2-carboxyethyl) phosphine (TCEP) for 1 hour, were then diluted to 5 M in 1× PBS and filtered with Zeba spin desalting columns (7K MWCO, 0.5 mL, Thermo Fisher Scientific AG, Reinach, Switzerland). This step insured reduced disulfide bonds. The leaning procedure was followed by denaturation of the aptamers (5 minutes at 95 °C). The last step was to wash out the previously immersed MBS with MicroFil tips and refill the pipettes with the denaturated aptamer solution prepared in step two for at least two hours. The nanopipettes are washed 3 times with PBS prior to measurement. Further adjustments to the protocol for better yield control are presented in the results section.

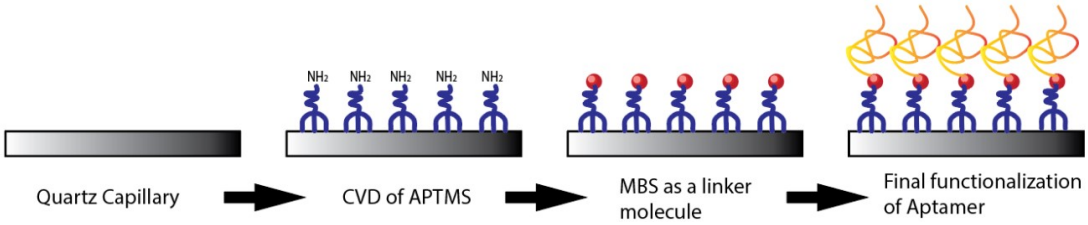

Figure 3.2: Functionalization flow schematic. In the ideal case, chemical vapor phase deposition of silane molecules results in monolayers, and thus the successive steps for aptamer functionalization are uniformly formed on the surface. The schematic is not to scale.

Dopamine preparation: Dopamine solutions are prepared with dopamine hydrochloride and ascorbic acid in excess to prevent polymerization. If not otherwise specified dopamine concentration of 100 µM is used to check the functionality of the aptamer. The previous students have proven no reaction of dopamine aptamer to the presence of ascorbic acid in excess (their results are unpublished).

Voltammetry setup measurement: Ag/AgCl quasi-reference counter electrode inserted inside a quartz pipette filled with PBS (see figure 2.2 (A)). The second Ag/AgCl quasi-reference electrode is placed into the bath containing the solution/cell of interest. The voltage of -0.5V is applied in the bath and the current versus time curve is traced until stability is reached. The cyclic voltammetry (CV) in the range (-0.7 : 0.3) V or (-0.5 : 0.5) with step 0.2 V/sec is performed to ensure the correct functionalization of the sensor and to check the stability of the current measurements. Most of the pipettes were pretested in PBS prior to the experiments. The protocol for pretest is the same as measurement one. Majority of pipettes tend to preserve current response after binding, thus decreasing reutilizaion of the pipettes. The updated washing protocol is present in the results section.

Data analysis: All the calculations, analyses, and plot generation were done by Python code written by A.Stuber with some custom modifications. The source is available at (`https://github.com/annaburds/DA_nanopipettes`).

3.3 Techniques

3.3.1 Quartz Crystal Microbalance with dissipation monitoring (QCM-D)

Quartz crystal microbalance with dissipation monitoring or QCM-D for short, is a highly sensitive mass balance that measures nanogram to microgram level changes in mass per unit area. The working principle is based on the thin quartz crystal disk sandwiched between two electrodes. Quartz is a piezoelectric material, - an applied electrical field will give rise to mechanical deformation and vice versa. When an alternating voltage is applied to the quartz crystal, it will oscillate back and forth.

Sauerbrey's equation. The relation formulated by Günter Sauerbrey so-called Sauerbrey's equation states if the sensor disk is loaded with a thin and rigid film of some material, where the film is tightly coupled to the oscillating sensor, there will be a proportional change (decrease in case of mass binding) in the sensor's resonant frequency, i.e. as mass is added or removed from an oscillating sensor.

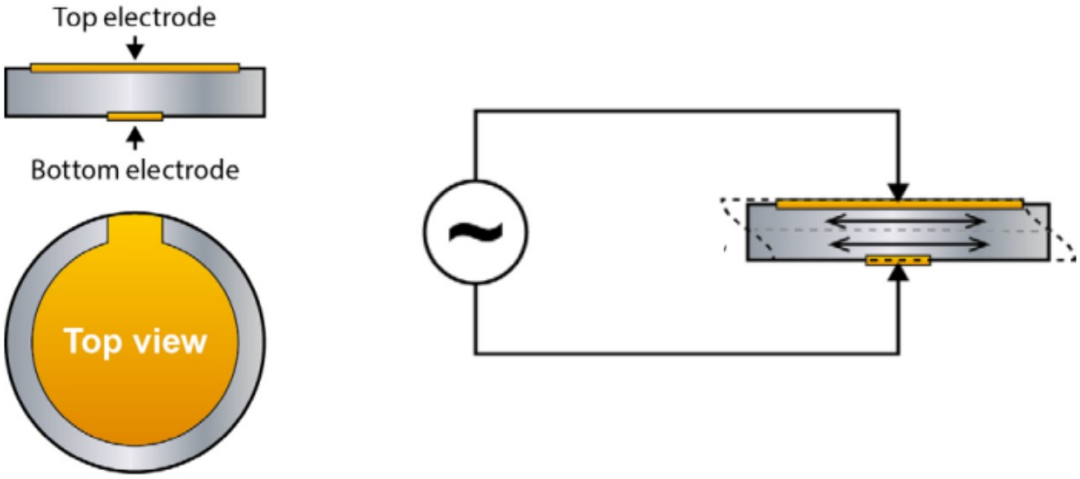

Figure 3.3: Left: Quartz disk sandwiched between the two electrodes. Right: Alternating voltage is applied, which causes the deformation of quartz crystals . At a certain frequency, f, the oscillating disk will be in resonance. Adapted from Biolin Scientific.

$$\Delta m = -\frac{C}{n}\Delta f$$

A change in mass - Δ m is proportional to the change in frequency - Δ f through mass sensitivity constant C = 17.7 ng/(cm ^{2} Hz) in quartz and overtone number n.

The model assumes that the adhered layer can be approximated to be a part of the oscillating crystal itself, which means that the crystal will have increased thickness. For this assumption to be valid, the layer on the sensor must be thin, rigid, and firmly attached to the crystal surface, and the equation should only be used when these conditions are fulfilled. If the layer on the sensor is soft, thick, or not coupled to the surface, the equation is not valid. In these situations, the model will fail, and the mass calculated with the Sauerbrey equation will be underestimated.

Additionally to the mass measurements, the QCM-D determines the dissipation (damping) factor. It is defined as the sum of all energy losses in the system per oscillation cycle and provides information about conformational changes and softness/rigidity (viscoelasticity) of the molecules studied. It can also be defined as the energy dissipated per oscillation, divided by the total energy stored in the system. With QCM-D, the dissipation factor is measured every time the drive generator output is stopped and the sensor oscillation starts to decay exponentially. A soft film attached to the quartz crystal is deformed during oscillation, which gives high dissipation. In contrast, a rigid material follows the crystal oscillation without deformation and consequently gives low dissipation.

Viscoelastic modeling. If the deposited layer is thick and/or soft and energy losses are not negligible, viscoelastic modeling should be applied for the computation of mass and height. The viscoelastic nature of the film needs to be considered otherwise film parameters provided by Sauerbrey's equation result to be underestimated. There exist several viscoelastic models [52], [53]. Typically the film is modeled as an elastic component in parallel with a viscous component, assuming homogeneous film density, thickness, and no-slip conditions [52], [54]. The information to be extracted from the measured values of frequency and dissipation change through a fitting routine is shear elasticity, shear viscosity, thickness, and density [55].

The experiments described in the result section do not provide numeric values of deposited mass and thickness due to variability obtained during parameters fitting. The approximation used to describe the results was to interpret frequency and dissipation curve deviation upon dopamine binding purely as a conformational change. The approximation is based on the evaluation of available binding sights of deposited aptamers and following calculation of maximum dopamine mass bound

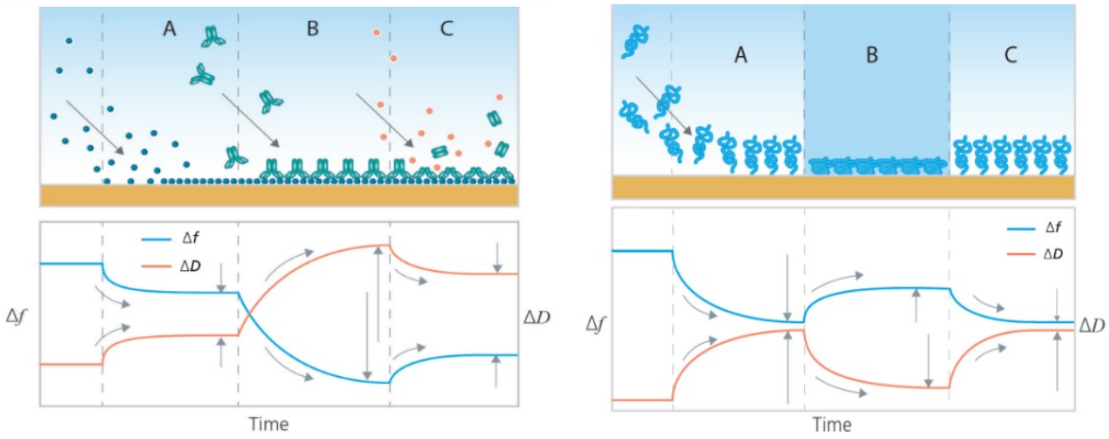

Figure 3.4: QCM-D output curves interpretation. **Left**: Different mass bound to the surface causes a different shift in frequency and dissipation (A-B). Binding of the mass to the QCM chip surface is characterized by the frequency decrease and dissipation increase. When the molecule unbinds the surface the opposite direction of frequency and dissipation is observed **(C)**. **Right**: Molecules binding to the surface are represented as a decrease in frequency and increase in dissipation**(A)**. Backbone reorientation into a more compact molecule causes frequency increase and decrease of dissipation **(B)**. In contrast, the opening of the DNA backbone is the reason for the decrease in frequency and increase in dissipation. Frequency can be seen as mass indicator, whereas dissipation characterize energy stored in the system. Adapted from Biolin Scientific.

(assuming 1x1 ratio), resulting in the negligible mass of the neurotransmitter with respect to the wet mass variability upon extension/contraction of the aptamers.

3.3.2 Standard addition

Standard addition is an analytical technique used to quantify the target concentration in a complex solution by minimizing matrix effects that interfere with analyte measurements. For the experiments in this present work, the solution with unknown dopamine concentration is diluted in PBS 100-fold (sample). Then, known dopamine concentrations are added to the sample: 1 pM, 5 pM, 8 pM, 10 pM, and 15 pM. These concentrations are taken from the nanopipette's dynamic range in PBS computed by previous student [56] (see figure 4.3.1). The first current recording is made in the PBS bath (no sample present) and is used later for normalization. The same pipette is used for the whole experiment. After normalization, the obtained values versus the concentrations of added dopamine are plotted. Linear fitting is applied and the intersection of the negative x-axis versus the fit line is the approximate concentration of dopamine in the sample. This concentration multiplied by the dilution factor (in this case, 100x) is the approximate concentration of dopamine in the solution of interest.

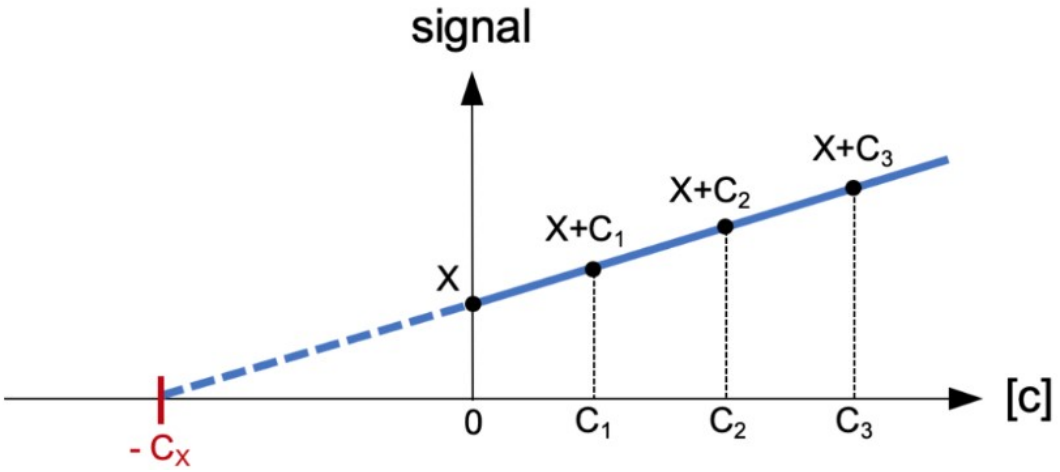

Figure 3.5: Standard addition method fitting curve. The normalized current response of a diluted sample of interest (X) and with added concentrations of the target molecule (Ci) are fitted into a linear model. The x-axis value at line intersection with y=0 (Cx) is the concentration of the diluted sample. Adapted from A. Failletaz Master's Thesis [51].

3.3.3 Focal Molography by Lino Biotech

Lino Biotech `https://www.lino-biotech.com` developed a novel chip architecture that can tackle various applications addressing major challenging points in cell and gene therapy. The core sensing technique is focal molography being nanotechnology-based method that combines photolithography, molecular self-assembly and state-of-the-art optical technology. Central to the technology is a biological surface structure termed mologram - biological diffractive element fabricated using biomolecules and nanolithography approaches. Biomolecules on the mologram detect the target analyte in the sample through molecular recognition and selective binding and thereby emit a light signal.

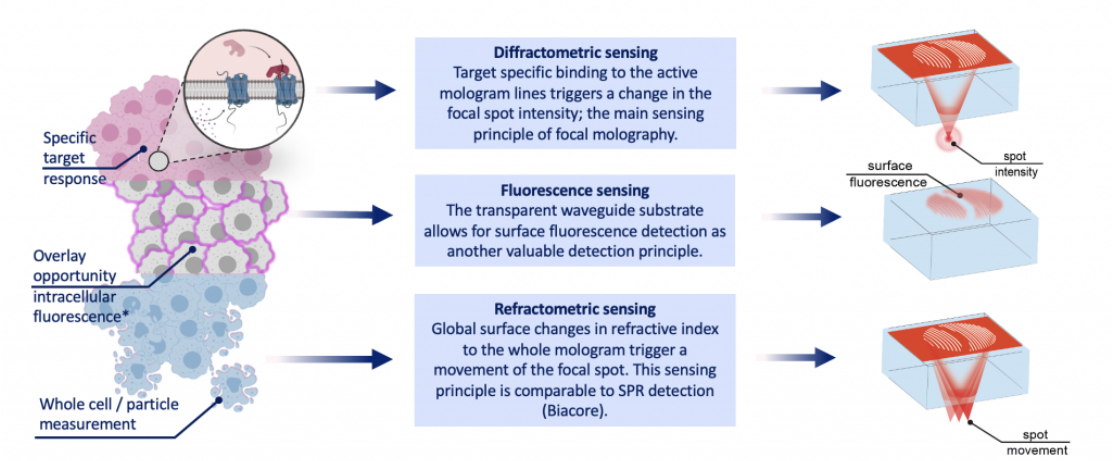

Figure 3.6: Lino Biotech chip applicability. The technology provides multidimensional data to characterize biological interactions. Focal Molography is a unique physical principle to measure any kind of molecular interaction. Lino Biotech is focusing on the multiplexed characterization in real-time of unlabelled biological material in the bioprocessing sector, where a fast and stable detection in complex media is key. Adapted from `https://www.lino-biotech.com/technology/`.

Lino Biotech provides its customers with mologram chips and reading setup. The chips utilized for the dopamine specific aptamers characterization has 54 mologrames functionalized on a single chip. By means of the complex chemistry (`https://www.lino-biotech.com/streptavidin-sensor-chips/`) aptamers layers can be deposited for further tests.

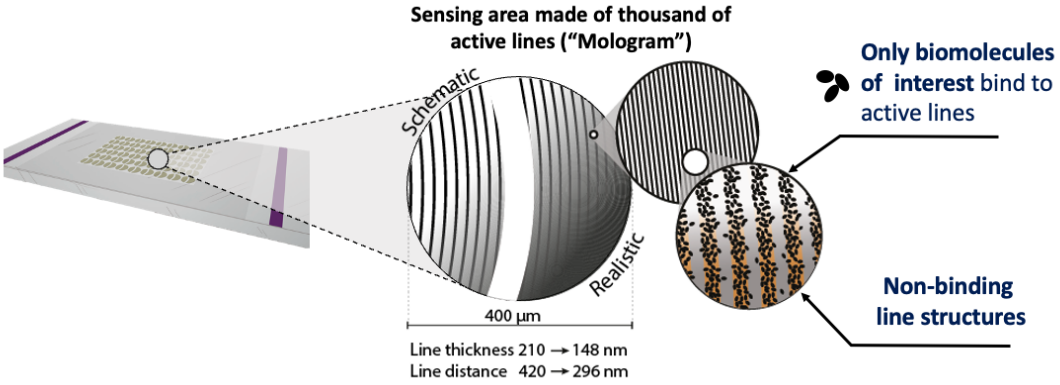

Figure 3.7: Working principle of mologrames. The mologrames are illuminated by a laser beam travelling from left to right across the chip surface. If light encounters biomolecules specifically bound to the active lines on the surface, it is diffracted into a focal point below the chip that can be measured. Adapted from `https://www.lino-biotech.com/technology/`.

Chapter 4

Results

4.1 Aptamer Characterisation

Previously developed serotonin nanopipette sensor showed an increase of current as a response to target binding [29] (see figure 4.1). This tendency is contrary to the one observed in dopamine-specific nanopipettes (see figure 2.2) and the difference in their behavior is hypothesized to lie in the opposite direction of the aptamer's conformational change. In order to find the origin of the dopamine nanopipette current response, a QCM-D characterization was performed.

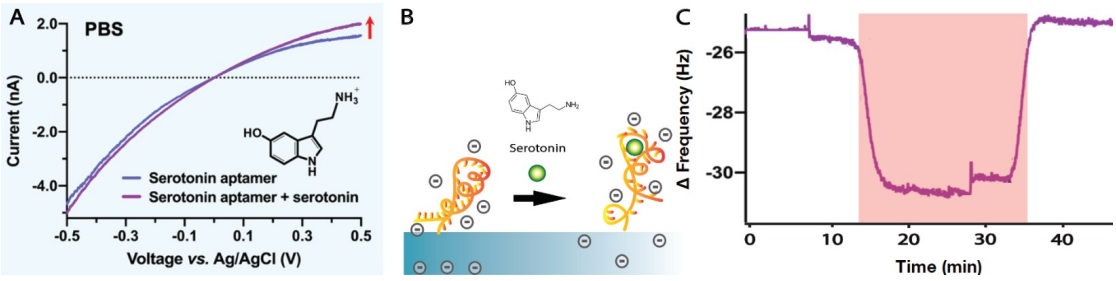

Figure 4.1: Serotonin aptamer performance characterisation. **(A)** Upon binding with serotonin nanopipette's ionic current results in an increase of amplitude. **(B)** Serotonin aptamer is assumed to undergo backbone reorientation causing depletion region on the deposited surface. **(C)** QCM-D frequency shift down can be explained by gaining of wet mass by absorbing surrounding water molecules of the aptamer upon recognition of the target. Pictures are adapted from [29].

Aptamer assembly. First, the aptamer was deposited on the gold chip to prove the functional thiol group that is responsible for binding with the MBS linker molecule (see figure 3.2). The green region on the figure 4.2 represents the

time when an aptamer-containing solution was injected. Following injection of PBS did not alternate frequency value and thus frequency decrease was due to the stably bound aptamers. Average viscoelastic mass value was used to estimate approximately the number of available binding sights, which for the present QCM-D round was of the order of 10^{13}. It means that 10^{13} dopamine molecules or around 3 ng/cm^2 could be rigidly attached to the QCM-D chip surface though aptamer bond. The maximum possible distinguishable frequency shift due to the deposition of this amount is less than 0.8 Hz, which is barely recognizable from noise for a 5 MHz quartz crystal chip`https://www.biolinscientific.com/measurements/qcm-d`). This information is useful in order to understand the origin of curve shifts, i.e. if it is due to the bound/unbound of mass or due to the backbone reorientation - wet mass alternation. In presented experiments, the shifts upon addition of dopamine are due to the conformational change, since the maximum frequency change due to the dopamine mass deposited can be considered negligible with respect to the wet mass alternation.

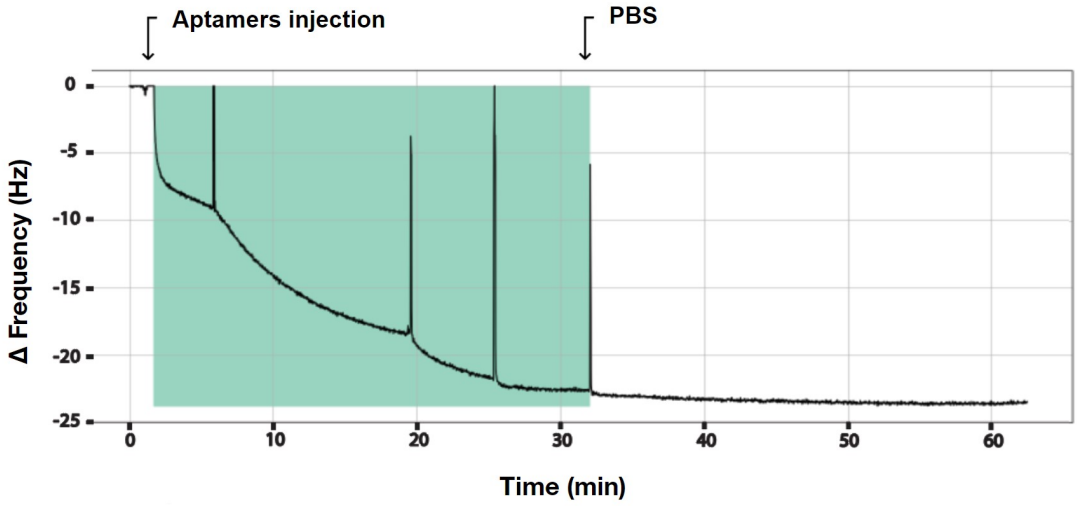

Figure 4.2: QCM-D frequency response upon injection of aptamer solution onto the gold surface chip. Successive washing with PBS ensures stable bond between the gold chip and thiolated dopamine aptamers. More binding curves can be found in supplementary information (see figure A1).

Dopamine induced backbone reorientation. The next step was to inject PBS containing 100 µM dopamine. The addition of dopamine resulted in an increased frequency and decreased dissipation, which can be interpreted as aptamer contraction. As it was mentioned in the method section (see figure 3.3.3), when a molecule, in this case, single strain DNA, shrinks, it releases water molecules

surrounding the backbone, thus decreasing wet mass. Aptamer structural switch into a more compact form brings a negatively charged backbone closer to the surface and in the case of nanopipette, such a change in charge distribution on the surface could be responsible for decreased conductivity. Interestingly, for N=¾ it was not possible to wash away the dopamine, i.e. it was not possible to reset to the initial frequency/dissipation values prior the addition of the dopamine by further injection of PBS. The same behavior of non-resetability was observed in nanopipette experiments (see figure 4.3 C).

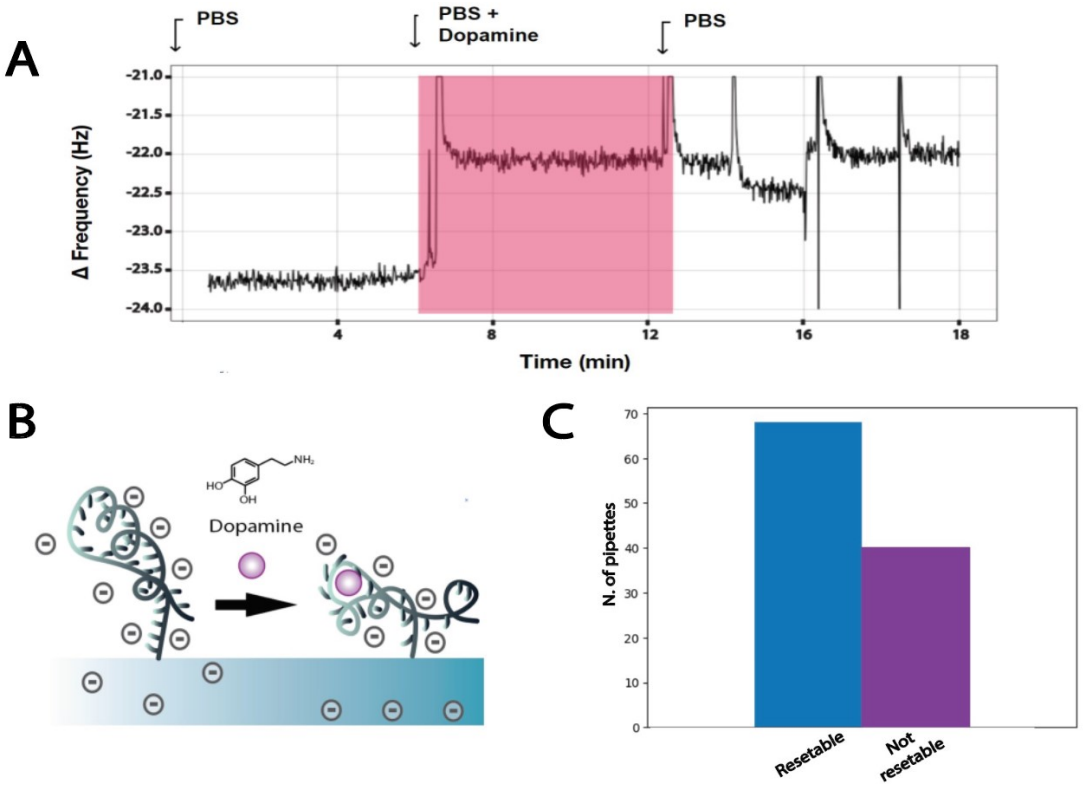

Figure 4.3: **(A)** QCM-D frequency response upon injection of PBS containing dopamine. The frequency shift upwards is due to the folding of the aptamer backbone, i.e. reducing the wet mass attached to the chip. The following washing step with PBS is not successful. **(B)** Possible conformational change direction of the dopamine specific aptamer. It is assumed that aptamer undergoes folding backbone switch bringing negative DNA backbone to the quartz nanopipette surface, thus alternating surface charges, which can be sensed with ICR. **(C)** Number of resettable nanopipettes versus not resettable in PBS from 1/10/22 until 17/7/23.

NaCl washing protocol. Several experiments were conducted in order to establish a washing protocol. It was observed that high concentration (mM - M range) NaCl and following PBS injection resulted in returning to the initial frequency and dissipation values, i.e., before the addition of cations and/or dopamine. This reversible experiment led to the hypothesis that salts were able to wash away dopamine from the aptamer backbone by introducing free ions being able to destroy dopamine-aptamer bonds and bring aptamers to initial conformational change. However, high concentration salts could damage the DNA molecules themselves, thus reducing the surface density of aptamers. Moreover, this washing approach does not apply to nanopipettes for several reasons: in addition to possible aptamer reduction on the surface due to the backbone destruction, high concentration salts could affect the quartz capillary of the nanopipette by etching the orifice pore or by clogging it with salt crystals. The washing protocol employing NaCl can not be used in cells and brain tissues, since it does not allow continuous resettable measurement. All in all, high concentration salt washing protocol is not applicable for nanopipettes but can be exploited for aptamer characterization experiments and less fragile sensing setup resistive to high salt concentrations.

Alternative washing methods with a salt composition closer to physiological fluids as well as purified water containing minimum/no ions were tested.

	PBS	aCSF
NaCl	137 mM	127 mM
KCl	2.7 mM	1 mM
KH_2PO_4	1.8 mM	1.2 mM
$NaHCO_3$	-	26 mM
Na_2HPO_4	10 mM	-
$CaCl_2$	-	2.4 mM
$MgCl_2$	-	1.3 mM

Table 4.1: PBS vs aCSF salt composition.

Divalent Cations. Divalent cations such as Mg^{2+} and Ca^{2+} have a specific influence on the aptamer as was previously seen by N. Nakatsuka et al. [27], [31]. The experiments performed on transistors showed that upon addition of both divalent cations to the buffer solution (PBS) aptamers undergo conformational change even in the absence of dopamine. The following addition of the target resulted in a bigger structural switch than was observed in PBS. Interestingly, two opposite behavior with divalent cations were recorded during QCM-D experiments.

First, the solution with divalent cations (PBS + 1mM $CaCl_2$ + 1mM $MgCl_2$ or aCSF) when inserted on top of the dopamine bounded in PBS resulted in a big frequency shift up. When later dopamine was injected cation-containing solution, a further upward shift was recorded. Similarly to the pure PBS injection after dopamine, it was not possible to reset QCM-D by washing dopamine away with the following aCSF injections. Neither injection time, volume nor speed affected the tendency of frequency response. There are two possible theories on that: first - the aptamers were bonded too tightly and thus their structural switch is limited by their density; second - there should be a change in a buffer solution in terms of ion concentrations in order to weaken interactions between aptamers and dopamine molecules, for example, wash with high-purity water (Milli-Q water - MQW). This assumption was successfully tested in nanopipette experiments.

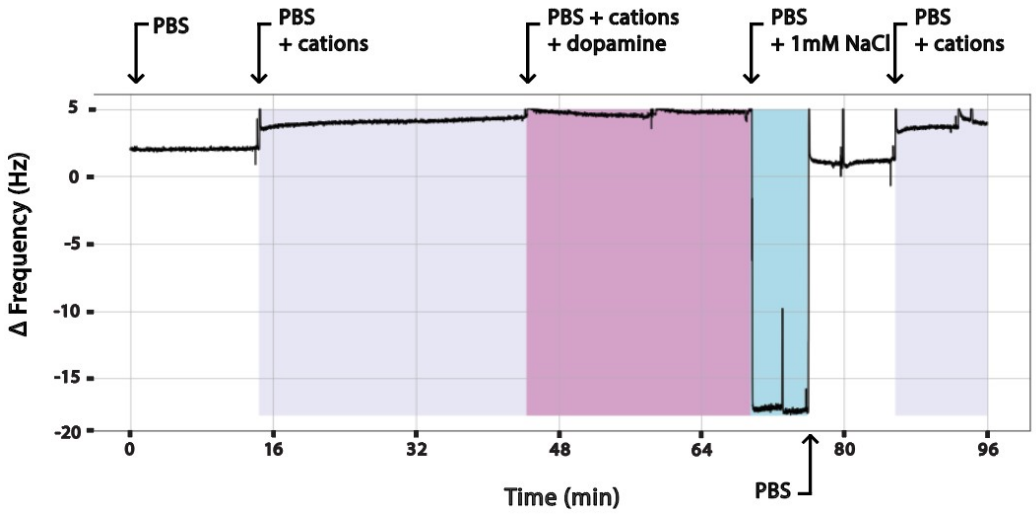

Figure 4.4: Influence of high concentration salt on the dopamine aptamer. Dopamine was injected on top of PBS solution containing Calcium and Magnesium cations and successive washing step with 1mM NaCl resulted in reversible frequency value. This frequency shift down can be associated with unfolding of the dopamine aptamer with the release of bound target.

When aCSF was injected after aptamer deposition, an increase in frequency due to bath exchange is twice less than when dopamine in PBS was pre-bound. Next, when dopamine is added to aCSF a negative shift of frequency occurred which described unfolding structural switching, opposite to what was initially expected. Moreover, this cycle was resettable (see figure 4.5). These observations are important however more experiments should be done in order to be able to

claim certain backbone reorientation directions in the presence of ions. It is possible that salt proportions play a crucial role in aptamer reaction to the target molecules.

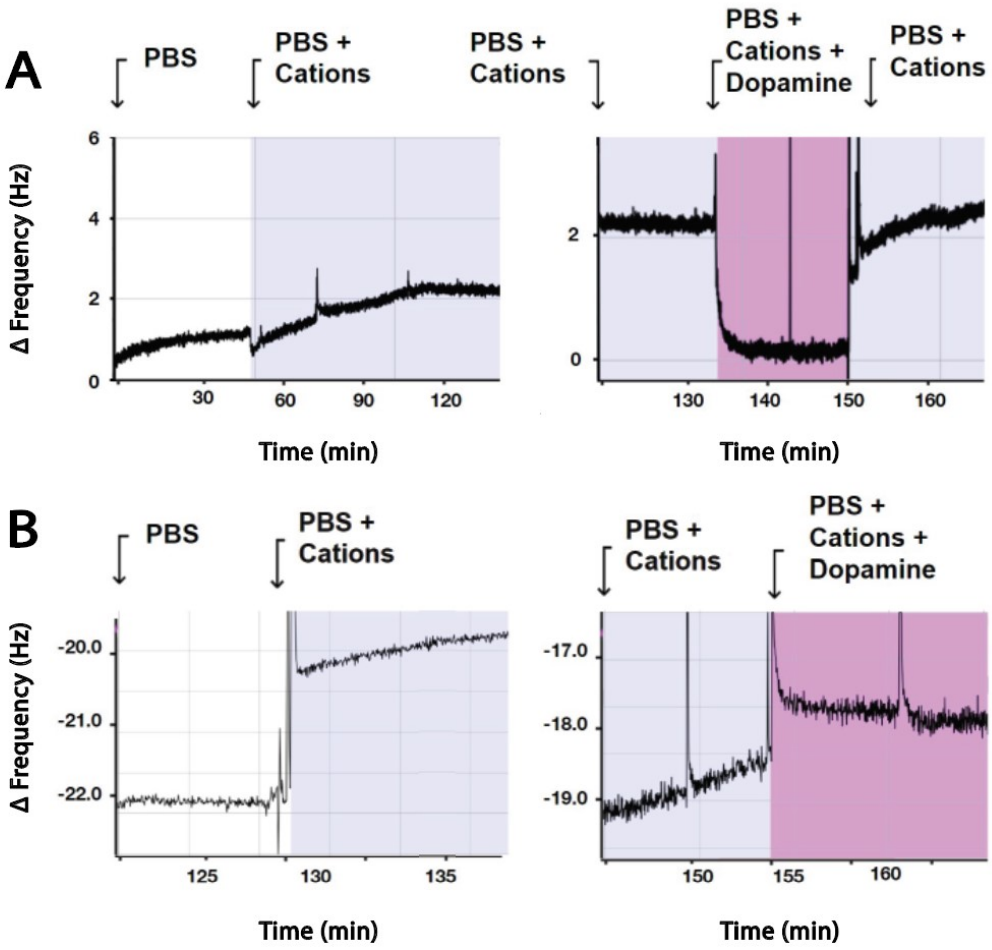

Figure 4.5: Two QCM-D rounds with similar deposited aptamer masses. **(A)** Left: When aCSF is injected to the QCM-D chip with deposited aptamers, frequency shift of Δ 1 Hz is observed. Right: Upon addition of dopamine the QCM-D result suggest unfolding conformational change of dopamine aptamer which is opposite to what is observed in PBS. Moreover, the conformational change is reversible upon washing with aCSF. **(B)** Left: aCSF is injected as the next step depicted on figure 4.3-A. Frequency shift is Δ 2 Hz and following injection of dopamine results in further upward shift. The injections of the described experiment were not reversible (see supplementary for the full trace of experiment). More experiments need to be conducted in our to obtain statistically relevant information regarding the aptamers conformational change.

Scrambled aptamer. In parallel, the experiment with scrambled aptamer was performed. Scrambled aptamer has the same length and weight as a dopamine sensing element, but the order of acid building blocks is different with respect to the target-specific aptamer. This sequence change makes scrambled aptamer not reactive to the target, i.e. no structural switch is observed upon molecule binding. Scrambled aptamer showed no reaction to dopamine when the buffer solution was PBS. However, when the experiment was conducted in aCSF the frequency shift occurred with the same amplitude and direction as dopamine aptamer in aCSF (see supplementary A6).

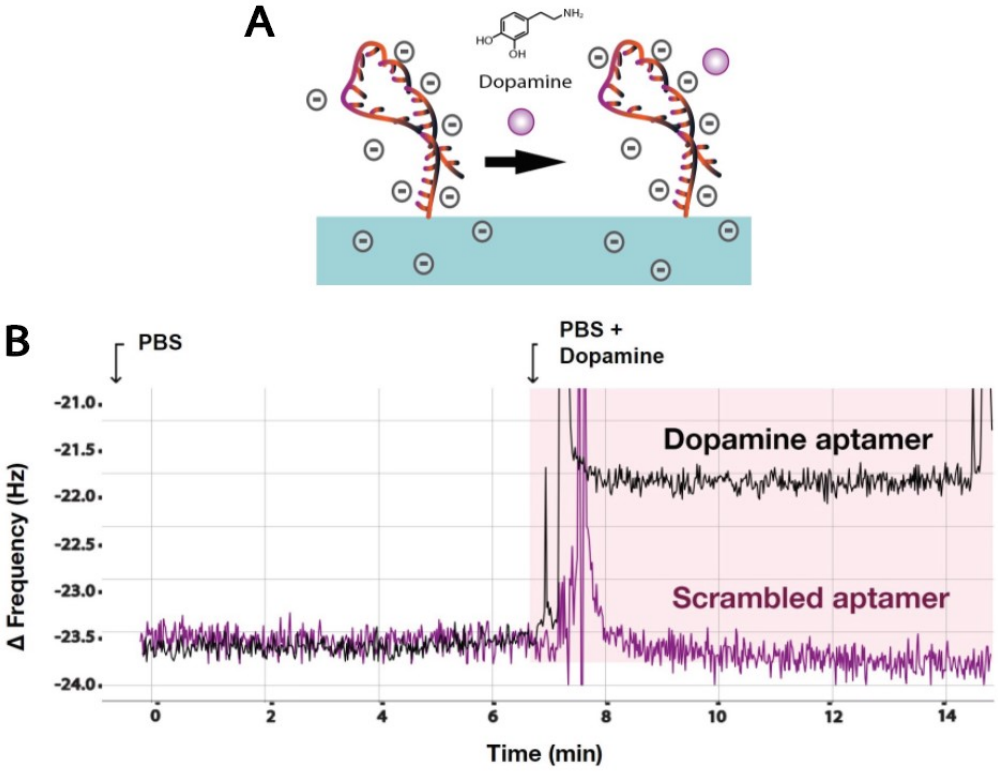

Figure 4.6: Scrambled aptamer. **(A)** When target molecule is present in the solution, scrambled aptamer does not change its shape. **(B)** Scrambled aptamer has shown no reaction during QCM-D experiment in PBS.

To conclude this section, dopamine aptamer undergoes a folding conformational change upon binding with the target when the addition is performed in PBS. However, depending on the ions present in the solution and starting backbone shape, the further structural switch has a different direction. Thus, one needs to

perform more experiments to identify the precise behavior of aptamer in presence of dopamine.

4.2 Lino Biotech. Dopamine aptamers characterization by means of molography.

An entirely new method was tested in order to characterize aptamer-target interaction. Lino biotech developed a nanotechnology-based method for measuring molecular interactions in living cells or crude biological samples that cleverly combines photolithography, molecular self-assembly, and state-of-the-art optical technology (see section 3.3.3). The core of the technology is a biological surface structure termed mologram - biological diffractive element fabricated using biomolecules and nanolithography approaches (molecules + hologram = mologram).

This technology offers label-free detection assays while eliminating signal disturbances due to temperature changes or non-specific binding. Noise minimization makes mologram technology extremely attractive for experiments conducted with aptamers, which can cause uncertainty in already existing characterization methods such as QCM-D. However, compared to QCM-D, Mologram technology sense only dry mass and is believed to be not capable of conformational change characterization. For this experiment slight modification of the aptamer's backbone structure was introduced. The experiments were conducted on the already predeveloped tetrazine-based chips (see methods and https://www.lino-biotech.com/ for more information), and since the goal of the experiment was to use the most stable bonds, for the role of linker molecule was chosen mono-streptavadin and aptamers were ordered with biotin instead of thiol binding group.

The aim of the experiment was to test the applicability of the mologram technology to the aptamers characterization. Figure 4.7 represents the output of 1 chip having 54 diffraction patterns (every mologram has its own focal point enabling parallel label-free multiplexing). Obtained results showed the possibility to detect and quantify aptamers stably bound to the surface of the chip. Successive injections of PBS and PBS+ dopamine solution did not introduce any significant signal. This absence of reaction was concluded to be due to the sensitivity limits of Mology chips. The signal detected in aCSF + 10 mM dopamine could be due to the buffer change, some bonded mass of the chip since the density shift was too high for single dopamine binding and thus could not be associated with pure aptamer-molecule interaction. More experiments were conducted with Lino chips, however, due to the development difficulties and lack of time no complete characterization of aptamer-dopamine interaction was done.

Today it is assumed that Lino biochips are not capable to detect tiny molecules such as neurotransmitters, however aptamers interactions can be successfully studied with higher mass molecules.

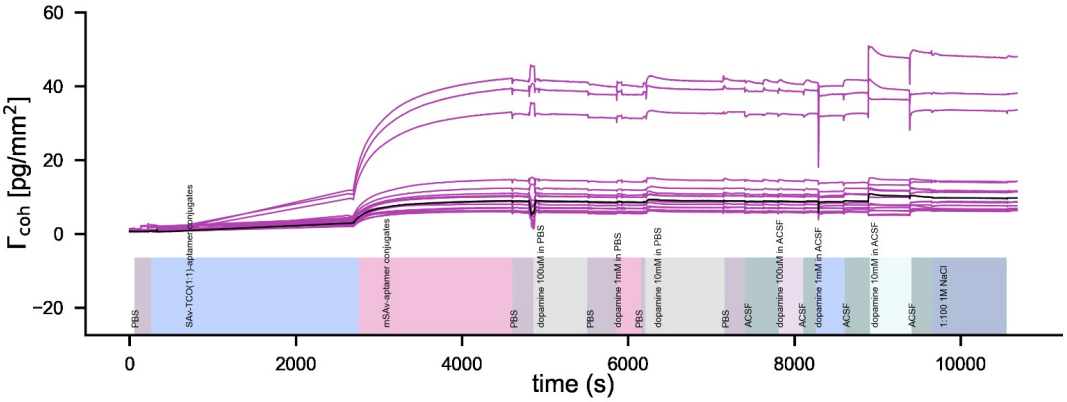

Figure 4.7: Mologram signal indicates the exact measure of binding affinity between recognition site and analyte in Γ [pg/mm^2] over time. Each line represents a signal from a separate diffraction pattern funtionalized on the chip. Aptamers can be successfully bond to the chips surface and successive binding is analysed. The introduction of different salts as a buffer solution results in a minimum signal perturbation. Lino biotech chips could not detect dopamine binding to the surface due to sensor's mass sensitivity, thus bigger mass has to be bond prior to the target.

4.3 Complex Matrices

Dopamine like other neurotransmitters can be found both in the brain and body fluids. The ability of the sensor to identify and correctly quantify dopamine in a complex environment such as neurobasal medium and blood serum can be of interest for pharmacological tests, and medical and biotechnology research applications. The main difficulties lie in the selectivity of the sensor in complex media, as well as its sensitivity. Dopamine-specific nanopipette sensor has high selectivity over similarly structured molecules such as L-Dopa, and norepinephrine due to the functionalization of nanopore surfaces with artificial recognition elements termed aptamers. However, the nanopipette performance also depends on the ionic concentration of the measured solution as well as its viscosity due to the nanoscale dimensions of the sensor. The experiments conducted previously with the dopamine nanopipette had shown the possibility to detect dopamine in PBS and neurobasal medium.

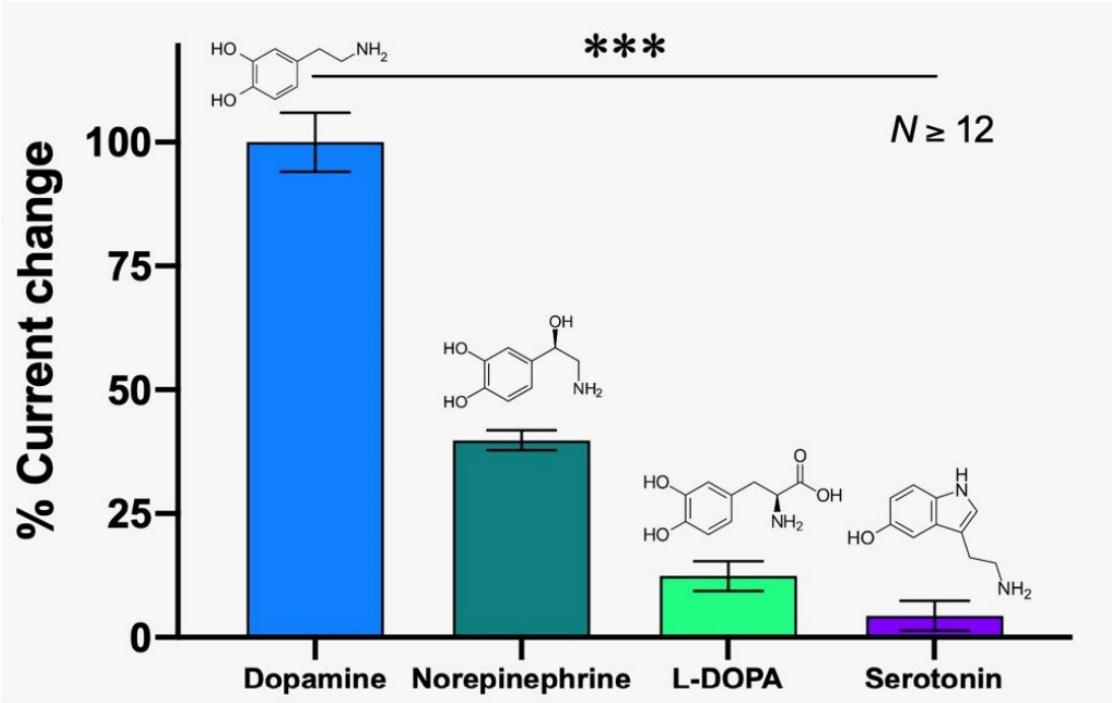

Figure 4.8: Selectivity of dopamine specific nanopipette sensors. The investigation of the nanopipette response to similarly structured molecules such as norepinephrine, L-DOPA, serotonin resulted in statistically relevant differences. Norepinephrine, which is the nearest related neurochemical to dopamine, evokes a response to a certain degree, which can be explained by aptamers selectivity over the whole molecule structure. Concentration of all the solutions are the same 100 µM. Adapted from [56].

4.3.1 aCSF

Artificial cerebrospinal fluid (aCSF) is a biological buffer solution prepared with a composition representative of cerebrospinal fluid that enables a vital environment for neuronal tissue by maintaining homeostasis, osmolarity, and pH at physiological levels. ACSF is commonly used to maintain vital conditions for the neurons (`https://en.wikipedia.org/wiki/Artificial_cerebrospinal_fluid`), thus the ability to detect dopamine in it opens space for the bottom-up study of neuronal networks, experiments in brain slices and more. Even though aCSF and PBS are quite similar in most of the salts concentrations (table 4.1), the divalent cations presented in the first buffer bring issues to the nanopipette performance (figure 4.5). Interestingly, when the reaction of dopamine nanopipettes was compared between the two buffers the divalent cation solution was not leading to a straightforward conclusion on its tendency. The minority of pipettes had an increase in current upon the addition of dopamine and were resettable afterwards without a further washing step, which is in agreement with the latest QCM-D results. At the same time the majority of pipettes, resulted in the same direction in aCSF as in PBS (see figure 4.11). Up to now, the core mechanism influencing such a diversity in current response still stays uncovered. By analyzing and comparing [56], [51], [57] (see figure 4.3.1) the LOD of dopamine pipette in aCSF and PBS it is possible to conclude that presence of ions does not significantly alter the Kd of the sensor. It is strongly advised to conduct more experiments to increase iteration number and obtain statistics with both PBS and aCSF.

4.3.2 Blood Serum

Despite the fact that dopamine can not cross the brain-blood barrier, many research teams [59], [60], [61] try to establish the correlation between neurotransmitter concentration in brain fluid versus human blood serum. The serum is the fluid and solute component of blood that does not play a role in clotting. It is obvious that the collection of blood serum requires less intervention and has minimal effect in comparison to brain fluid extraction. However, the quantification of dopamine in serum by means of nanopipette is not straightforward. Like all physiological liquids, the serum does not have constant ion and protein concentration over time. There are many factors affecting the serum composition such as hydration level, time period of the day [62], gender [63], age [64], etc. As was discussed previously (see chapter 2), the nanopipettes are extremely sensitive to the salt composition of a buffer solution (see figure 4.12), moreover, the serum has a higher viscosity index, and thus dilution can be necessary to avoid pore clogging. To check the applicability of the nanopipette in serum samples the two solutions were tested interchangeably: diluted serum samples with and without 100 µM dopamine. The primary results showed the possibility to detect high concentrations of dopamine

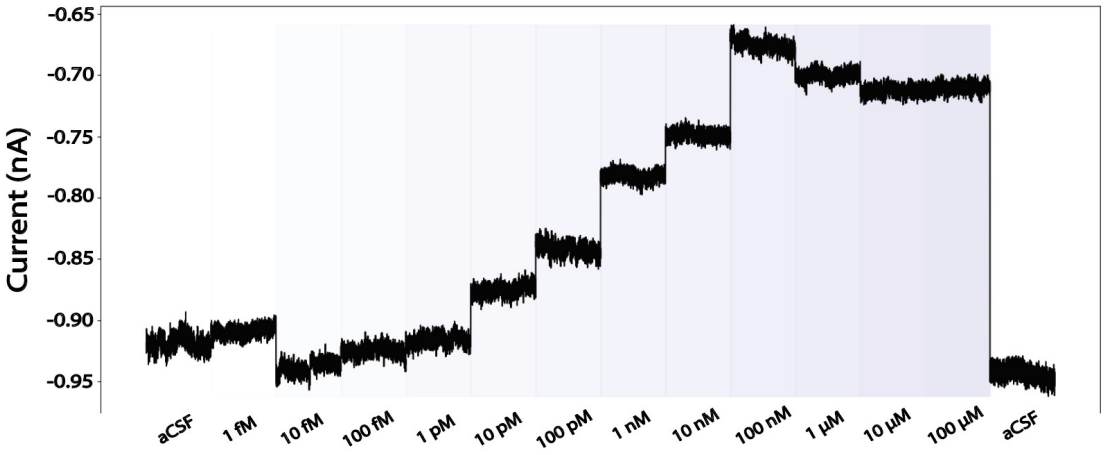

Figure 4.9: Nanopipette current (decreasing) response to the increasing dopamine concentration in the aCSF.The measurement is not performed real time and signal was performed after 10 CVs and recording was done for the next following 5 minutes until stability is reached. The last aCSF recording was made after nanopipette washing with PBS. Important to notice that current response of the nanopipette usually decreases during the first few measurements (aCSF-> 1 fM ->10 fM). This tendency is clear on this graph however it is general for all the nanopipette experiments: freshly made nanopipette needs bath exchanges/wash/time to reach its maximum value, thus there is always uncertainty for the first nanopipette measurements.

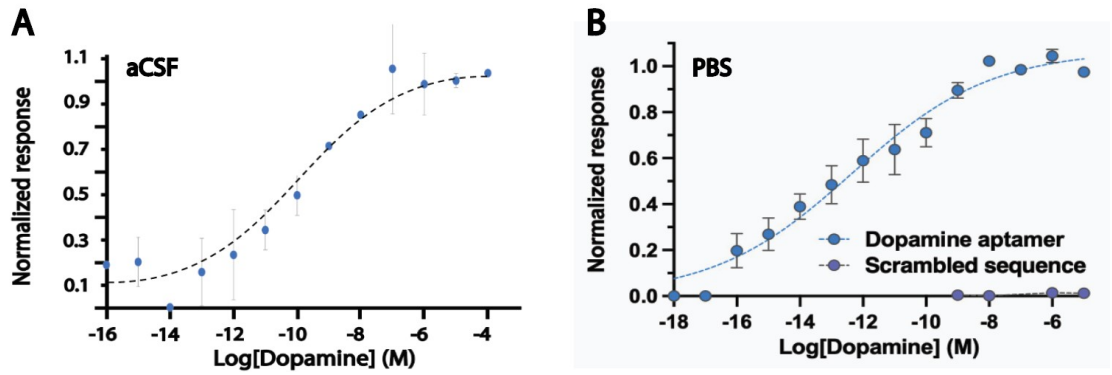

Figure 4.10: Calibration curve of dopamine specific nanopipette sensor in aCSF **(A)** and PBS **(B*)**. In accordance with the statement above first few measurements of nanopipettes in aCSF results in a values smaller than expected in absolute value (lower concentrations has higher current than higher concentrations). * is adapted from [56], [58].

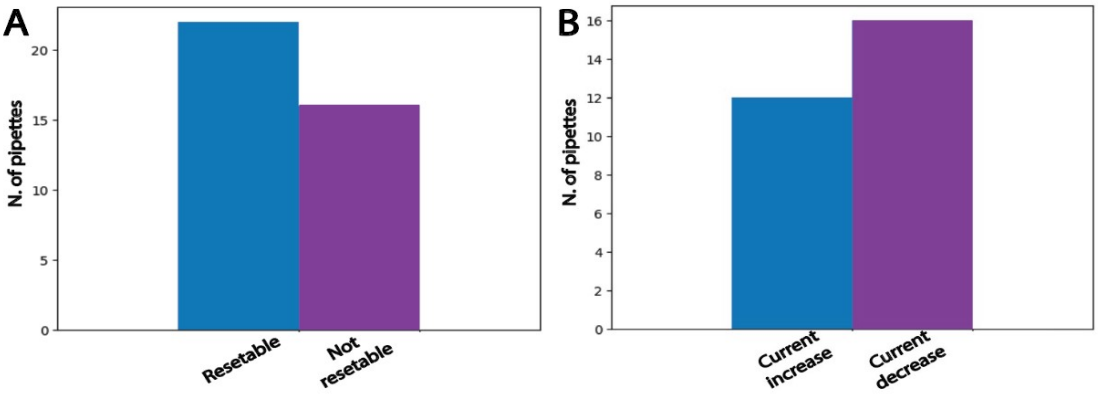

Figure 4.11: Statistics of the dopamine specific nanopipette performance in aCSF collected during whole duration of Master's Thesis Project. **(A)** Resetability of aptamer embedded nanopipettes. Similar to PBS bath, after dopamine binding in aCSF solution nanopipette had to be washed with MQW or PBS. The not resettable pipettes statistics was collected without washing protocol. **(B)** in aCSF nanopipettes have different tendency upon binding to dopamine. Statistics represent the reactive sensors that were either resettable with and without washing protocols.

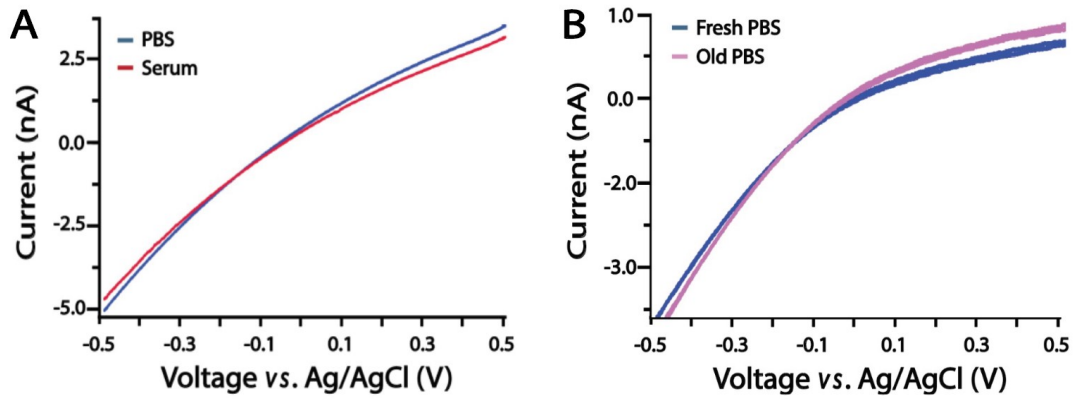

Figure 4.12: Buffer composition influence on the nanopipettes performance. **(A)** Same pipette has different current baseline in PBS and serum. Serum was not diluted and decrease in conductivity could also be due to the higher viscous index with respect to PBS. **(B)** Evaporation causes higher ion concentration per unit volume which can be represented as current increase. Old PBS stays for the solution of 500 µl stayed for 15 min. in the room with open cup. 500 µl fresh PBS was taken from the same stock as the old one, but was measured immediately.

within the sample (see figure 4.13). However, future experiments would require a parallel measurement with a control (scrambled) sensor in order to get rid of all the matrix effects of the environment, which are unavoidable for more advanced *in-vitro* experiments.

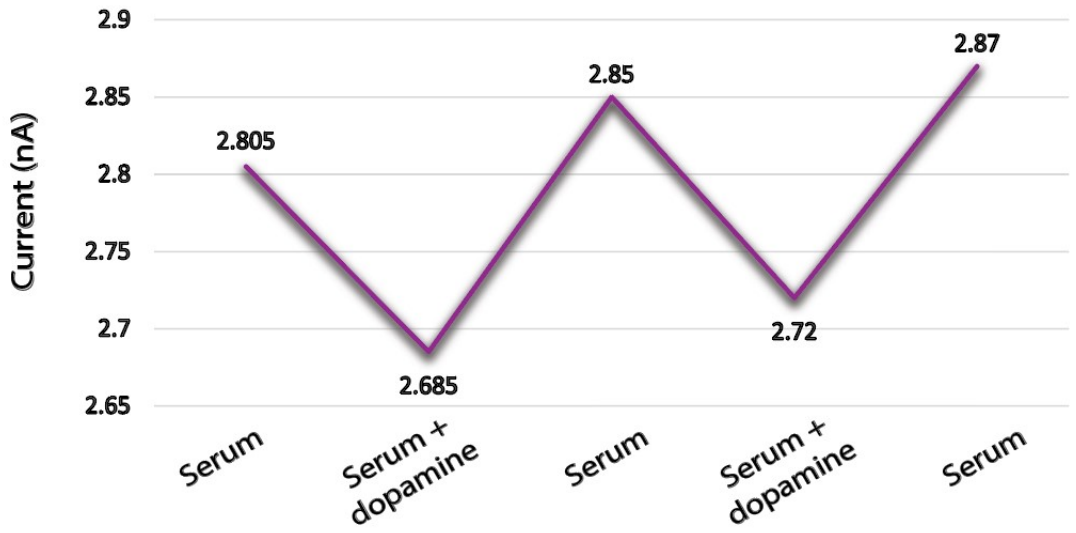

Figure 4.13: Dopamine detection test in blood serum. Average values of the real-time measurements image resetability of the pipette. Moreover, the observed drift upwards can be explained by evaporation, i.e. increase of salts concentration in the buffer solution.

4.3.3 Clinical Samples

The ability of the sensor to identify and ideally quantify dopamine in a complex environment is essential for medical and research applications. Our collaborator - iXCells Biotechnologies is a cell biology and cell technology company focusing on preclinical drug discovery on cell models. Among other neuron cultures, iXCells derive dopaminergic (iDa) neurons (see Supplementary A9). One possible way to check the function of iDa neurons is to detect dopamine in the matured cell culture medium. Moreover, precise dopamine quantification can be used as a characteristic evaluating drug performance.

A.A. Manole initially provided us with three samples: a neuronal medium buffer solution from the stock (no neurons were grown in the solution), a neuronal medium of the motor neurons grown for 7-day (which was used as a negative control), and

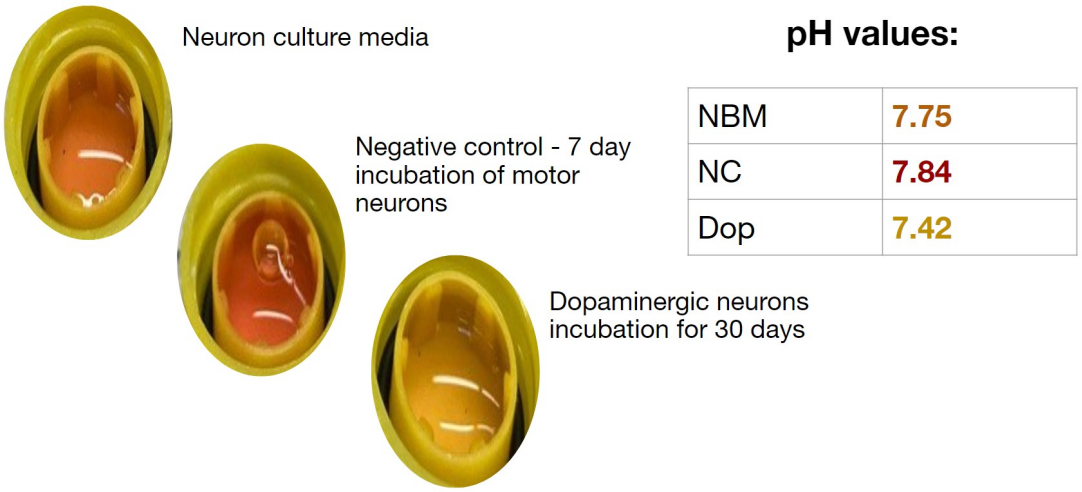

Figure 4.14: Neuron culture media provided by iXCells biotechnology. The three samples had different composition and, as it was tested later, different pH values. The two samples Negative control and dopaminergic (iDA) neurons media were used for further experiments.

neuronal medium dopaminergic neurons grown for 30 days (see figure 4.14). Samples were frozen at -80 °C and delivered to the laboratory where the experiments with nanopipettes were performed. The three samples had different colors, and pH values, and when the pretest was done, all three had completely different ionic content (see supplementary A). In order to distinguish between current alternation due to medium origin and dopamine concentration, the samples were tested with the dopamine nanopipette sensor and after with the scrambled nanopipette sensor. For the sake of simplicity, the comparison was performed between the negative control and the iDA culture medium. Since it was not possible to perform sensor versus scrambled nanopipette measurement contemporaneously some precautions were taken into account. First, due to the limited clinical sample volume available for the test (2 ml in total), the aliquots of 200 µl were used for each experiment round. One of the sources of ionic content alternation is evaporation. To preserve maximum possible ionic content, the ice was placed around the cups containing the samples during the measurement and the caps were covered with parafilm otherwise. The experiments were conducted with the same timing parameters, i.e. real-time recording was done over 5 minutes and CV was run for at least 10 cycles. The new sample aliquot was used for each series of experiments.

After implementing all the precautions listed above, the samples were tested. Even though the scrambled sensor was having a decreased tendency from negative control to iDa sample, the current drop observed in the sensor during bath exchange is noticeably bigger as depicted in figure 4.3.3 A (see supplementary for N=3 A). CV measurements resulted in an evident current drop sensed by dopamine specific sensor, whereas the control sensor response was due to the composition difference between the two samples. Normalization and subtraction of control value from the dopamine-specific sensor can be used for the concentration quantification. However, up to now, only a few data points were available due to the limited volume of clinical samples.

Several tries were attempted in order to identify approximate dopamine concentration in the iDa samples. The standard addition method was used with both PBS and aCSF. By the end of the master's thesis, it was possible to obtain correctly behaving N=2 for PBS measurements and none for aCSF, since the current tendency was not identical from batch to batch. The cause of such unpredictable behavior could be malfunctioning pipettes since some of them were not pretested prior to use. Standard addition conducted in PBS resulted in hundreds of picomolar concentrations of dopamine which is in accordance with expected values (see figure 4.3.3 B).

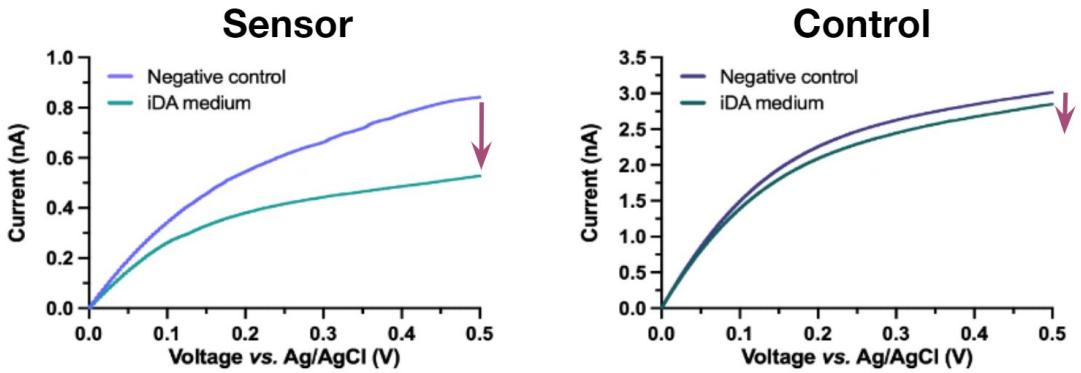

Figure 4.15: Comparison of CV curves between sensor and scrambled nanopipettes. Sensor has bigger current drop, whereas control represents the shift only due to the difference in ionic content. Both pipettes were resettable, excluding the drift current which could result in value decrease. The shown values are not normalised in order not to lose the control's change in current.

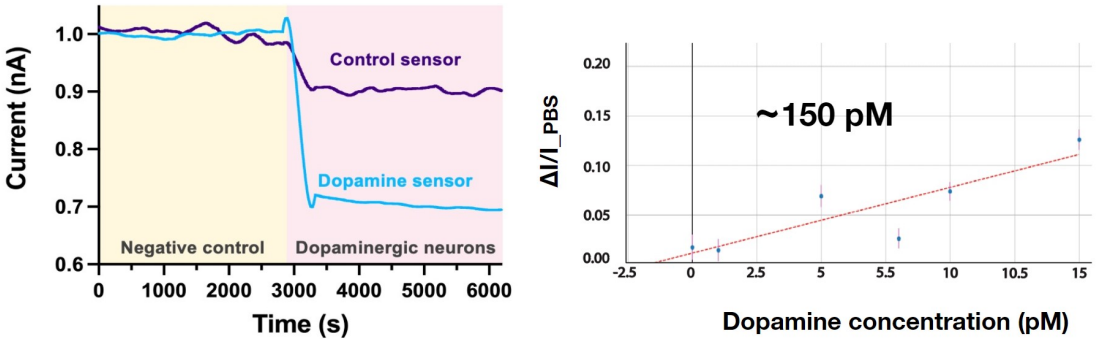

Figure 4.16: Clinical sample reaction pattern of dopamine specific sensor and scrambled sensor **(A)**. The decreased normalized current of the control sensor represents a conductivity alternation due to the difference of ionic content. During the experiment same media bathes were used and precautions were taken to avoid evaporation. More curves can be found in supplementary section. Standard addition experiment with N=2 results in approximately hundreds of pM concentration **(B)**. Standard addition experiment was decided to be performed with PBS due to the higher stability of aptamers compared to their behavior in aCSF measured during QCM-D experiments.

4.4 Tackling Reproducibility

In order to obtain scientifically relevant data, it is essential for the experiment to be reproducible - have minimum output alternation when parameters are kept constant. The repeatability of nanopipette experiments is tightly bonded to batch production. The first step as was described previously in methods is pipette pulling. During 6-month several capillaries batches from the same manufacturer were tested. Pulling time can be referred to the tip's orifice diameter and later on to the current amplitude in the measurements. Sometimes long pulling time was the reason for the extremely long tips with clogged or broken orifices, such pipettes were eliminated immediately. Even though precautions were taken, no significant changes were done to the protocol for this step.

The next step is silanization. Up to now, this is the least controlled step for pipette functionalization. J. Yota [65] revised that chemical vapor deposition of APTMS saline has significant advantages over liquid phase deposition. Among the advantages is the possibility of better control over thickness: CVD forms a uniform monolayer, and research [65] shows less compared to liquid phase dependence on humidity and temperature. However, obtaining such a result with a high yield becomes tedious when working on the nanoscale. Nanopipette tips require a nearly perfect monolayer in order to stay open and later successfully be functionalized with MBS linker molecule responsible for aptamers attachment.

From observation, humidity and temperature of the clean room affected batch production. One possible problem was hiding in the condensation effect. When a colder object is inserted into the high humidity warm environment water droplets are likely to be formed on its surface. In the case of silane, if it gets into contact with water molecules it undergoes polymerization. Thus any water droplets presented on the tip orifice most likely would cause clogged pores (see figures 4.4, 4.4). In order to avoid nano-droplet formation within the tip the first step was to introduce further humidity control by locating a dehumidifier and not performing any functionalization when the value of the relative humidity sensor surpasses 60%. Moreover, right before silanization, the pipettes were preheated up to 95 °C for 10 minutes. This way pipettes were equal to or higher temperature than the environment, thus reducing the risk of condensation and formation of nano-droplets responsible for silane multilayer.

Successive functionalization steps did not perturb any modifications except it was noticed that overnight incubation with aptamers and successive intense washing of the nanopipette with MQW led to higher performance.

Precise control over the humidity in a clean room, precautions against condensation, preselection of the pulled quartz capillaries, overnight incubation, and updated washing protocol led to the overall yield increase (see figure 4.4)

Figure 4.17: Clogged nanopipette with silane deposition on the inner nanopipette surface near the tip. The pipette was functionalized with relative humidity higher than 60% .

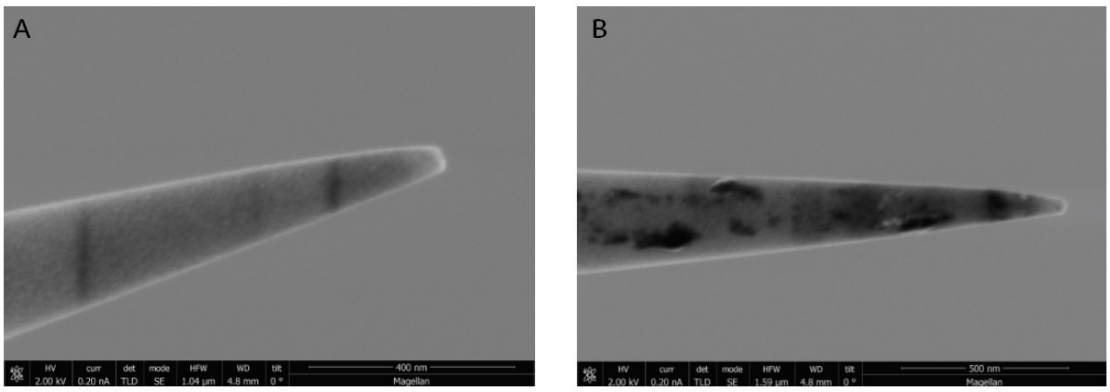

Figure 4.18: SEM images of the nanopipettes tips prior to functionalization **(A)** versus post functionalization **(B)**. Silane deposited on the outer nanopipette surface can cause contamination and further pore clogging. From the obtained picture **(B)** we can deduce small possibility of having monolayer saline. Pipettes were net tested prior to imaging.

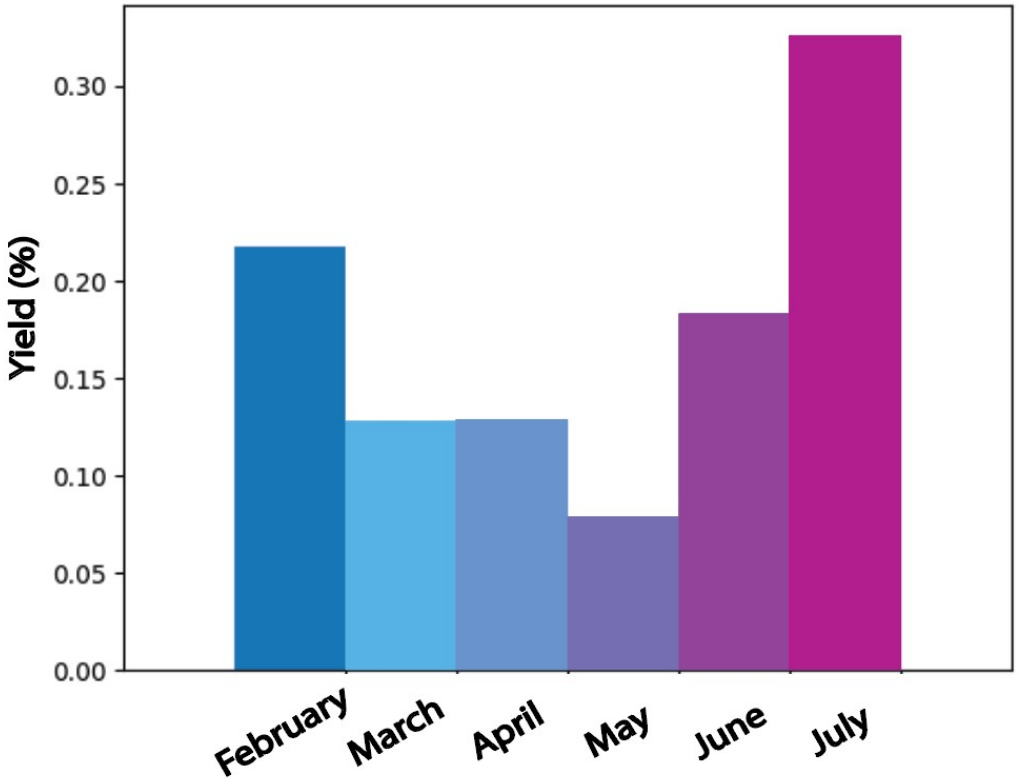

Figure 4.19: Percentage of working pipettes over total number of pipettes tested per month. Some pipettes were thrown away due to undesirable trend of the whole batch and those pipettes were not taken into account.Moreover, during yield estimation nanopipettes produced with visual defects were ignored. Primary statistics represents percentage of correctly working pipette during their pretest (resettable with the current decreasing tendency) even with small reaction amplitude over all tested pipettes of the month. From mid-May the adjustments to the protocol started to be implemented and by the end of July total yield per month became more than twice the one of spring.

Chapter 5

Conclusion and Further Perspective

5.1 Conclusion

The work carried on during the Master's Thesis was focusing on the characterization of the dopamine-specific nanopipette sensor and its core component aptamers. Previous research [58], [51], [56], [57] conducted on the same technology was able to examine the sensitivity and selectivity of the nanopipette sensor in PBS and neurobasal medium. During the last six months, it was proven that overall technology is working and the nanopipette sensor can be used to detect dopamine even in complex matrices such as blood serum and neuron culture media clinical samples. Moreover, the origin of the current response was analyzed. QCM-D studies revealed a folding direction of aptamers conformational change upon binding with dopamine in PBS. The presence of divalent cations strongly affected dopamine aptamer behavior and further studies are necessary for understanding the ions' influence on the aptamers backbone. An alternative sensing platform for molecule interactions was investigated. Mology experiments are fast and less subjected to noise, however, detection of small molecules such as neurotransmitters requires more sensitivity than existing chips can provide. Finally, several adjustments to the nanopipette functionalization and measurement protocols were introduced with the goal to increase overall yield. It was possible to reach a yield of more than thirty percent by introducing control over environment relative humidity, reducing condensation effect within nanopipette tip, and introducing washing protocol with MQW. Even though, the current nanopipette sensor is capable to perform successful dopamine detection in media of interest, scaling of the technology stays challenging.

5.2 Further Perspective

Measurements in clinical samples revealed the necessity to keep track of the environmental factors together with the target sense. A single nanopipette can reach synaptic range spatial resolution; utilization of the technology described in this work implies a control sensor as a separate pipette inserted in close proximity to the sensor pipette (see supplementary for the setup characterization A). Due to the nanometer scale, positioning of the control nanopipette next to the target-specific sensor stays challenging. One possibility is to develop a double pore nanopipette. Such a sensor would allow high spatial resolution measurements with an environment account.

Another crucial point to be introduced is new surface chemistry, which overcomes silanization limitations and thus would lead to a higher yield.

Appendix A

Supplementary

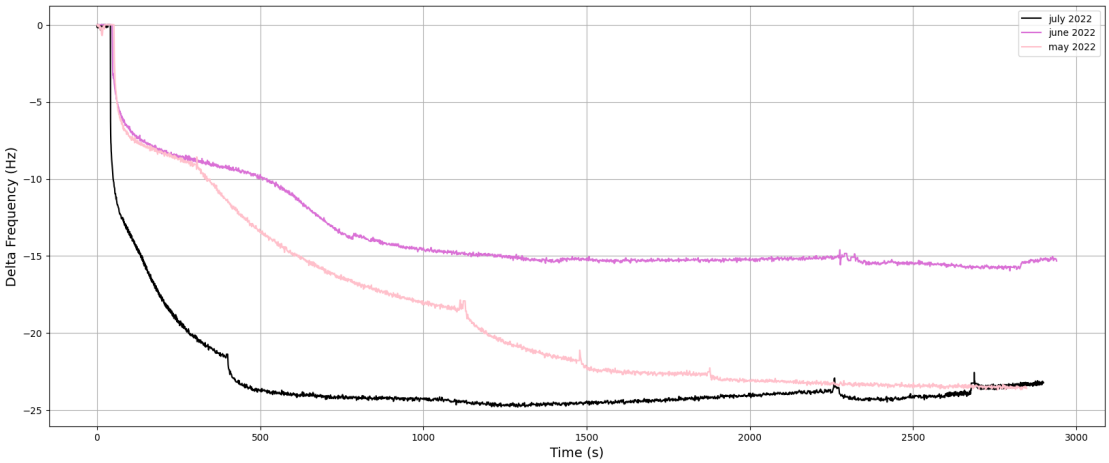

Figure A.1: QCM-D: Dopamine aptamers binding curve in PBS. Each experiment had different affinity and different total mass. Interestingly, nearly all bound mass was strongly attached to the surface chip, washing steps revealed no significant frequency alternation. No precise mass extraction was done from the viscoelastic model due to unreliable parameter dependence (tiny parameters perturbation was causing exaggerated mass values).

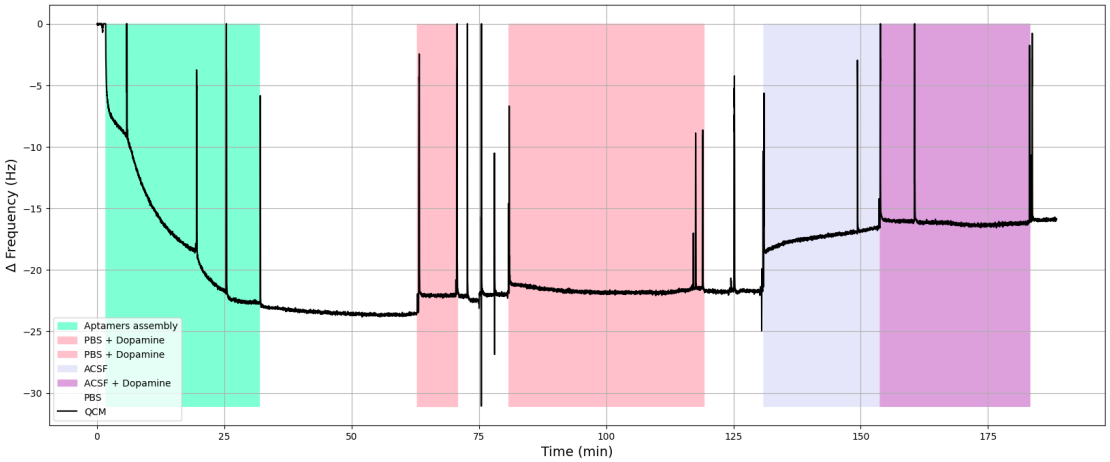

Figure A.2: QCM-D: Full QCM trace used as an example in results section. First dopamine addition was performed in PBS and resulted in positive frequency shift (dissipation curves are not plotted for the sake of clarity). following injections of PBS with the aim of washing of dopamine were not successfull. Second injection of dopamine containing solution was performed and no significant frequency alternation was noticed. Following hypothesis of improving washing protocol by addition of either higher salt concentration buffer or lower was tested. PBS solution containing 1mM $CaCl_2$ + 1mM $MgCl_2$ was added on top of unsuccessful wash with PBS. Frequency response upon addition of ions is 3 times bigger than upon addition of dopamine and can be explained in different ways: jump due to the buffer exchange, which has characteristic frequency drift; conformational change of dopamine aptamers with target bonded to the DNA backbone resulted in significant mass reduction + frequency drift. The following dopamine injection in cations rich solution resulted in a stable frequency curve with light shift upwards. This last phenomenon can be explained either by experiment instability either by dopamine binding to the available free aptamers. Following washing step was not successful.

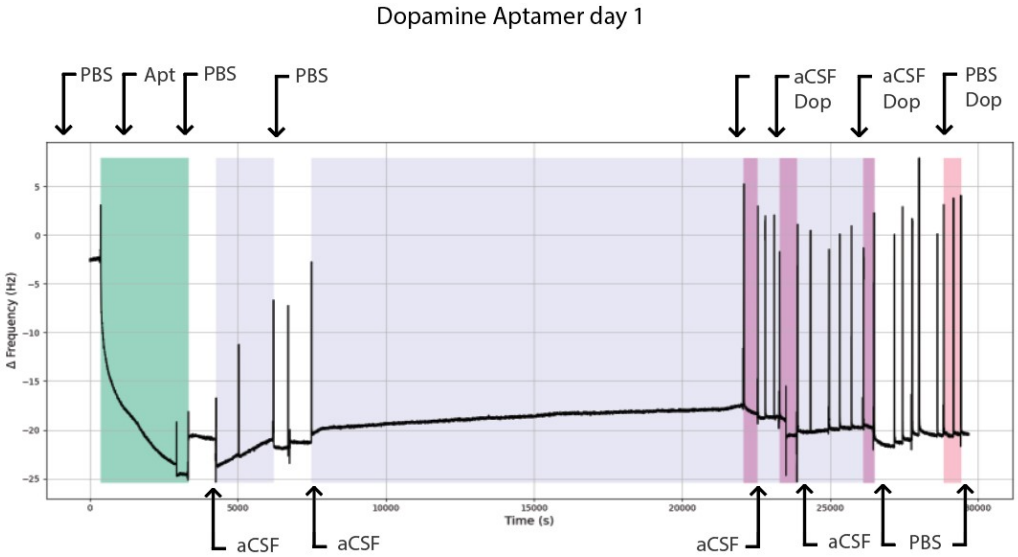

Figure A.3: QCM-D: The first day of the experiment described in the result session. The QCM-D experiment resulted in not stable frequency response upon buffers injections. Assumption of instability due to bath exchange was tested and system stayed for several hours in aCSF. However, following dopamine injections induced frequency decrease. The experiment run was conducted by A.Stuber.

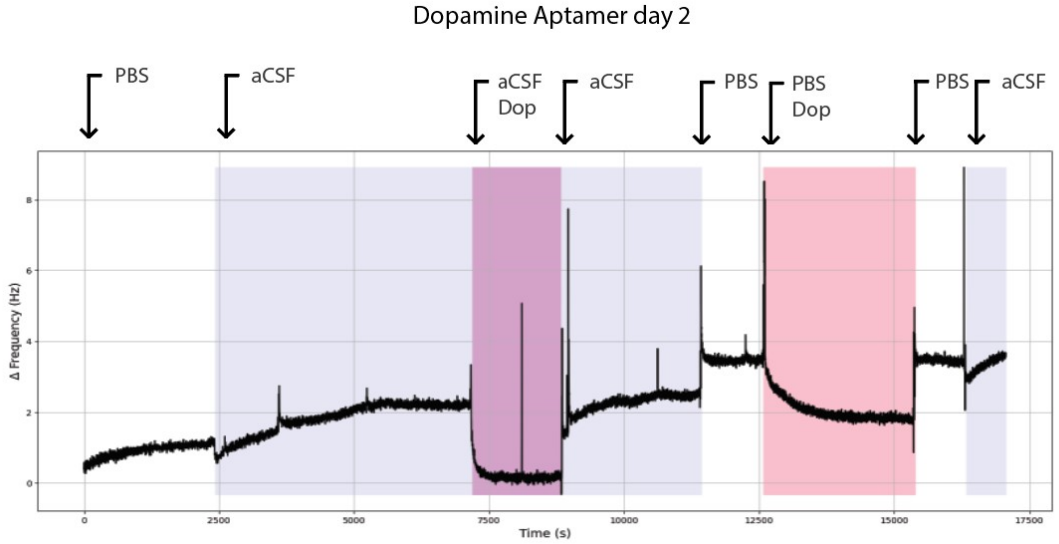

Figure A.4: QCM-D: Second day of the experiment described in the result section 4.1. The quartz chip was left overnight in PBS, several overnight PBS injection were performed in order to ensure complete washing of the aptamers.

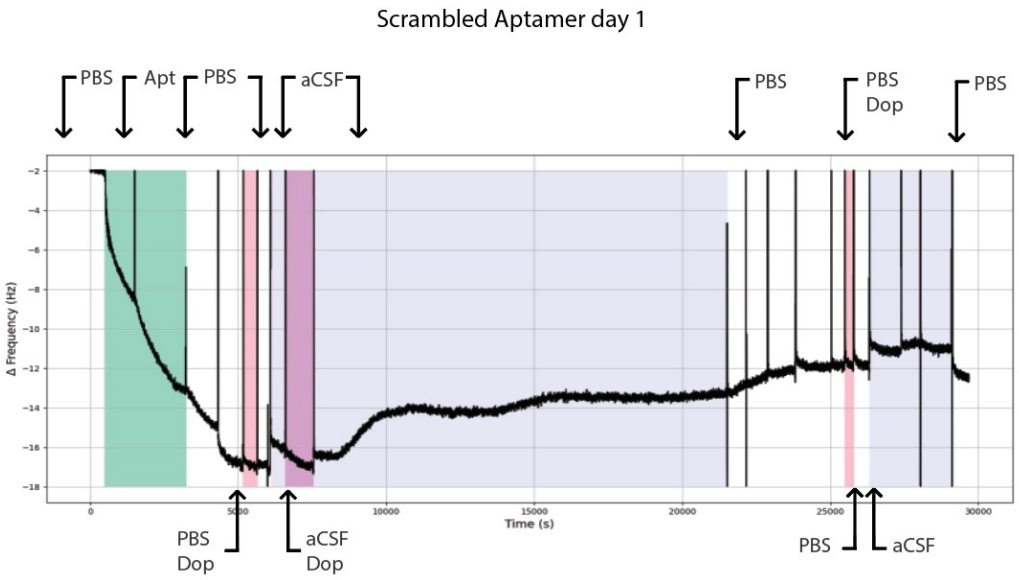

Figure A.5: QCM-D: Scrambled aptamer experiment day 1. QCM-D frequency curve results in instability upon aCSF injection. The system was washed with PBS and left overnight. The experiment run was conducted by A.Stuber.

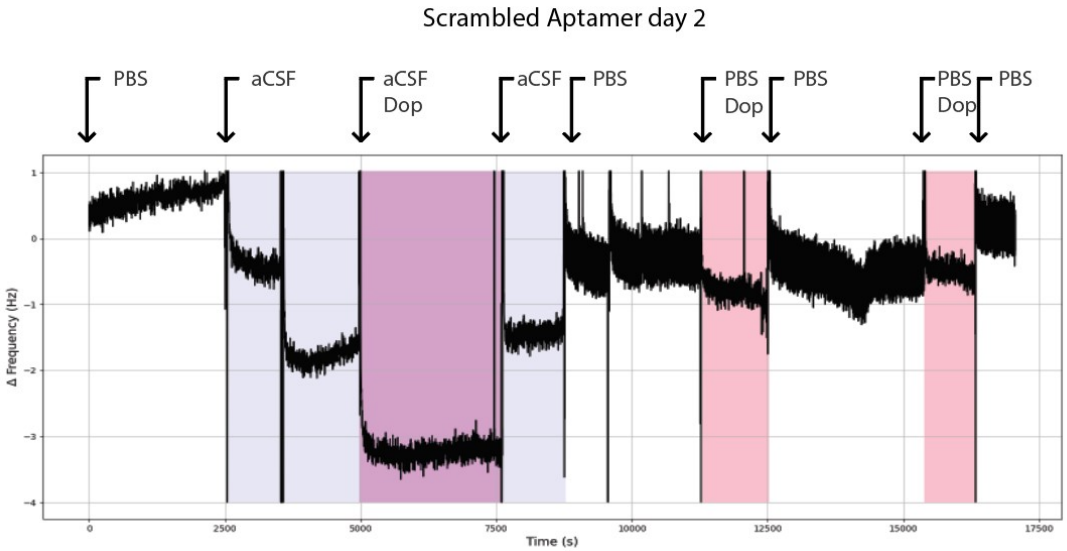

Figure A.6: QCM-D: Scrambled aptamer experiment day 2. After overnight incubation in PBS and visual stability for over 3 hours the system was washed with PBS. After PBS washing two consecutive aCSF injections were made. Each injection could be characterized by frequency drop and overall stability. Unexpectedly when aCSF + dopamine were present in the system, further frequency decrease was recorded. Any frequency drop is unexpected for scrambled aptamers, moreover the drop had same amplitude as dopamine specific QCM-D experiment described above. To check if scrambled QCM-D experiment was still accountable and working properly, following injection were done with PBS. PBS and PBS+dopamine curves had minimal difference in their response. Thus, we can conclude that scrambled aptamers requires more characterizations, ideally with different sensing platforms.

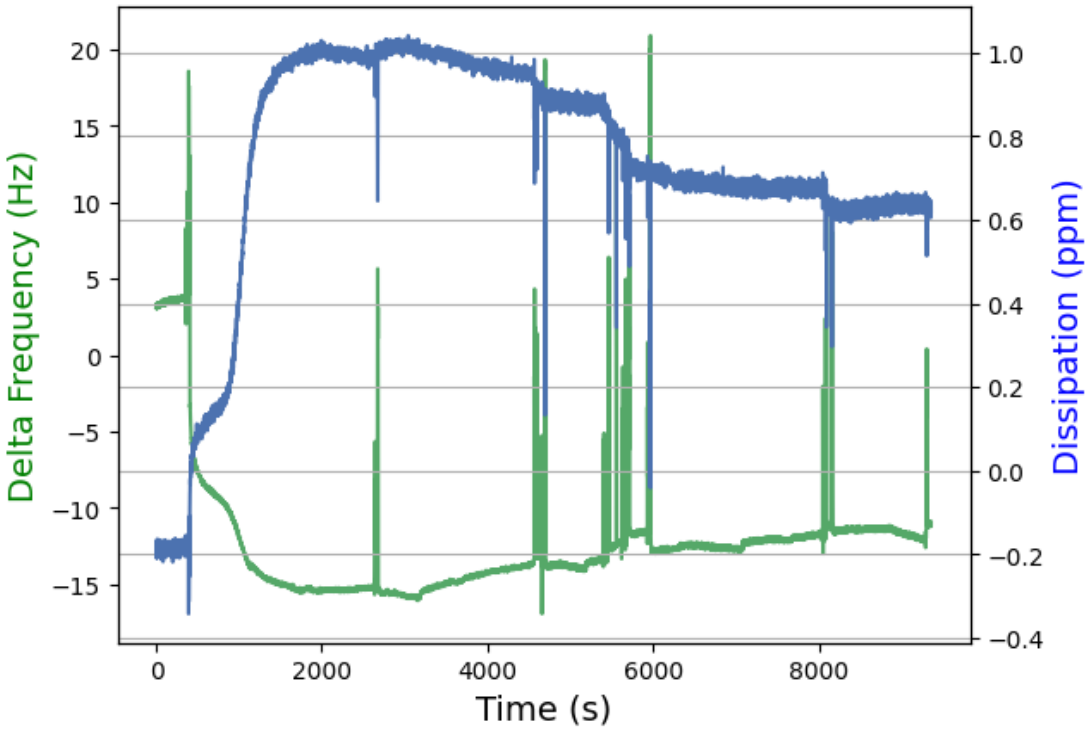

Figure A.7: QCM-D experiment with the need to use viscoelastic modelling due to wide span of dissipation values. Frequency and dissipation have opposite symmetric behaviour on different scales. The goal of experiment was to check stability of the sensor in presence of divalent cations.

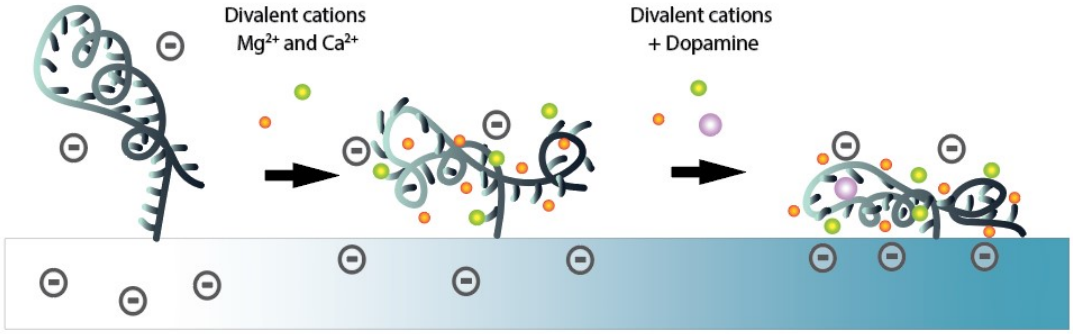

Figure A.8: Possible aptamers backbone reorientation due to the presence of divalent cations. Magnesium and calcium ions in media affect aptamers and cause reorientation of the DNA structure [27], [31], thus modifying the charge distribution on the surface where they are deposited. Following addition of dopamine assumed to result in folding aptamers structure, thus a significant conductivity drop can be measured with the nanopipette. Unfortunately, the model of dopamine aptamers behavior in the presence of ions is not that simple and further investigations are necessary.

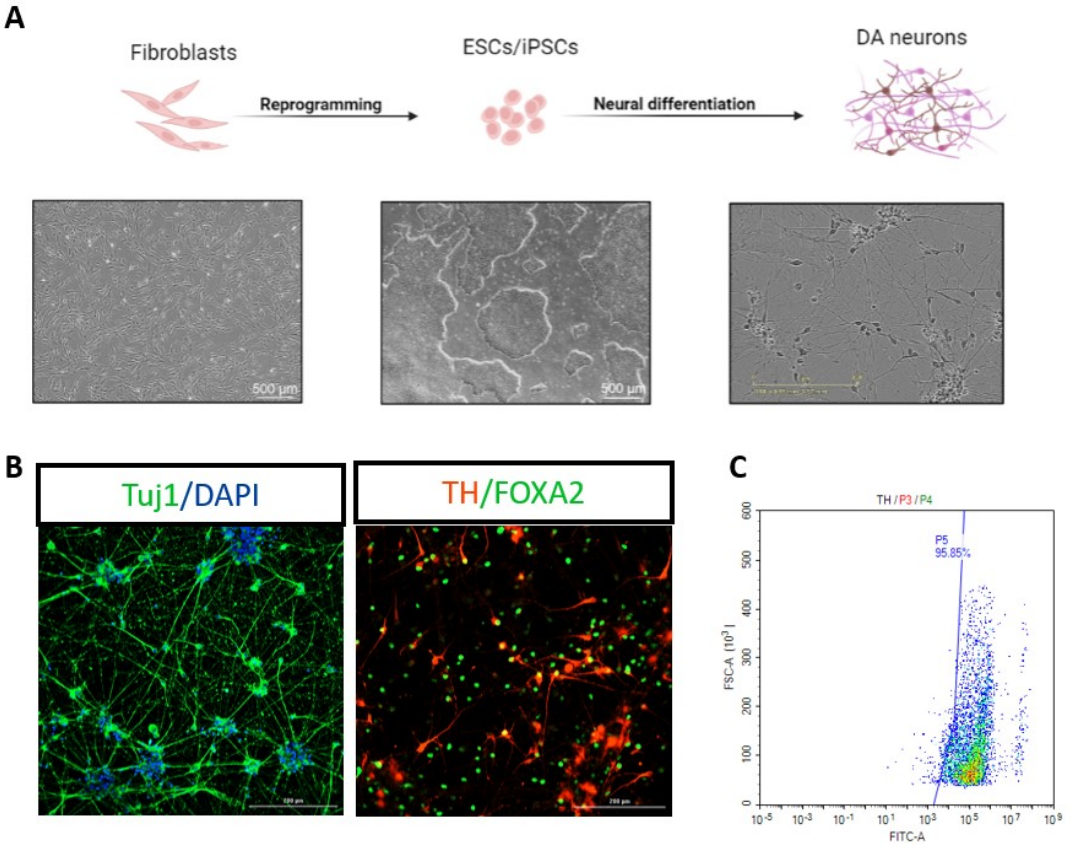

Figure A.9: **(A)** Schematic representation of the process of obtaining human iPSCs-derived dopaminergic (DA) neurons. **(B)** Human iPSCs derived dopaminergic neurons show expression of characteristic biological markers. Immunostaining shows the expression of neuron marker Tuj1 and midbrain dopaminergic neuron markers FoxA2 and TH, 28 days post-thawing. Nuclei were counterstained with DAPI. Scale bars, 200 µm. **(C)** Flow cytometry measurements demonstrate a highly specific population of fully differentiated midbrain dopaminergic neuron (TH).

Figure A.10: Normalized current response of dopamine specific and scrambled nanopipettes sensors. No noise filter was applied to the data. Experiments were conducted in turns, where indexes (sensor1 - scram1) represent the number clinical sample aliquot used. All dopamine specific sensors had higher current deviation compared to scrambled sensors. More experiments are needed to evaluate statistical difference between the two.

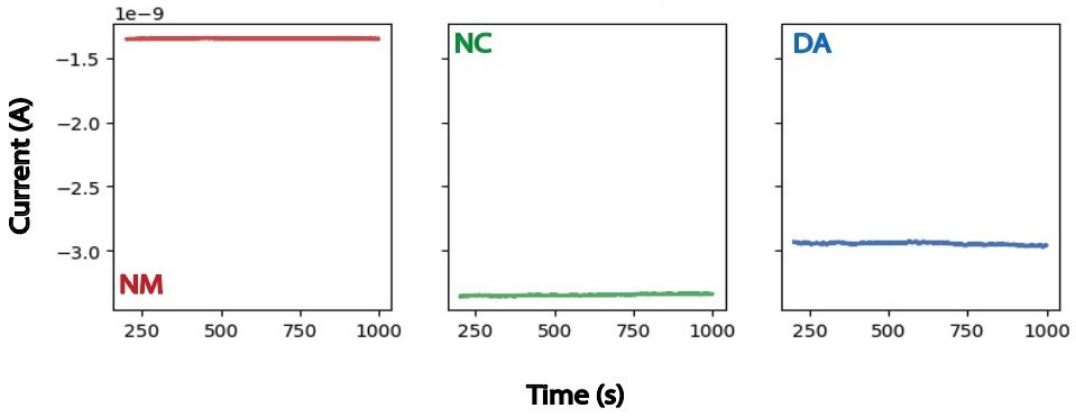

Figure A.11: Scrambled aptamer current response in three provided by iXCells clinical samples: Neuron culture medium from stock (NM), medium from motor neurons culture grown for 7 days served as negative control (NC) and matured dopaminergic neurons media (DA) have diverse ionic content which results in non identical current amplitude. The experiments were resettable with iteration number i=3.

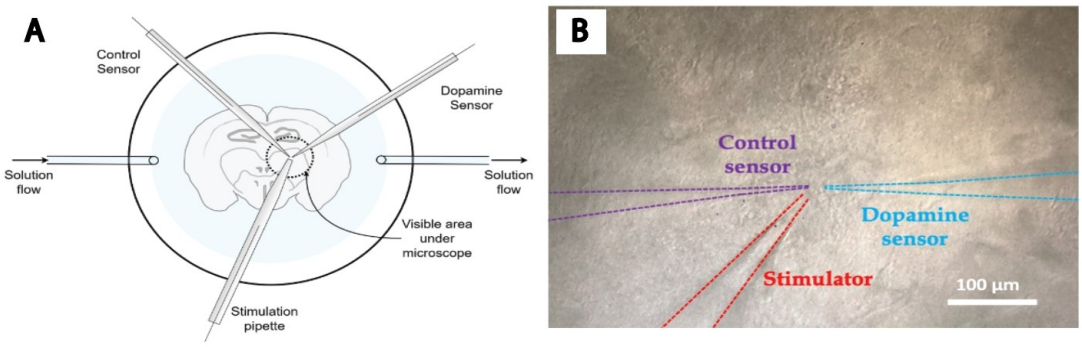

Figure A.12: Experimental setup for dopamine sensing performed ex-vivo. The measurements were performed on mice brain slices in the dorsolateral striatum. **(A)** A patch pipette, used for stimulating a brain cell and triggering dopamine release through a current application, was placed in close proximity to the dopamine and scrambled sensors. **(B)** Microscope image of the sensor placement. Adapted from [57].

Bibliography

[1] B. Güntekin E. Başar. «A review of brain oscillations in cognitive disorders and the role of neurotransmitters». In: *Elsevier BRAIN RESEARCH* (June 2008), pp. 172–193. DOI: 10.1016/j.brainres.2008.06.103 (cit. on p. 1).

[2] F. Mora et al. «Stress, neurotransmitters, corticosterone and body–brain integration». In: *Elsevier BRAIN RESEARCH* (Oct. 2012), pp. 71–85. DOI: 10.1016/j.brainres.2011.12.049 (cit. on p. 1).

[3] Leslie L Iversen. *Dopamine handbook*. Oxford University Press, USA, 2010 (cit. on p. 1).

[4] W EHRINGER. «Distributior of noradrenaline and dopamine in the human brain and their behavior in disease of the extrapyramidal system». In: *Klim. Wschr.* 38 (1960), pp. 1236–1239 (cit. on p. 1).

[5] Kenneth L Davis, René S Kahn, Grant Ko, and Michael Davidson. «Dopamine in schizophrenia: a review and reconceptualization.» In: *The American journal of psychiatry* (1991) (cit. on p. 1).

[6] Joshua D Berke and Steven E Hyman. «Addiction, dopamine, and the molecular mechanisms of memory». In: *Neuron* 25.3 (2000), pp. 515–532 (cit. on p. 1).

[7] Nele Plock and Charlotte Kloft. «Microdialysis—theoretical background and recent implementation in applied life-sciences». In: *European journal of pharmaceutical sciences* 25.1 (2005), pp. 1–24 (cit. on p. 2).

[8] Kerstin Buck, Patrizia Voehringer, and Boris Ferger. «Rapid analysis of GABA and glutamate in microdialysis samples using high performance liquid chromatography and tandem mass spectrometry». In: *Journal of neuroscience methods* 182.1 (2009), pp. 78–84 (cit. on p. 2).

[9] Barry L Hogan, Susan M Lunte, John F Stobaugh, and Craig E Lunte. «Online coupling of in vivo microdialysis sampling with capillary electrophoresis». In: *Analytical chemistry* 66.5 (1994), pp. 596–602 (cit. on p. 2).

[10] Mei-Yi Zhang and Chad E Beyer. «Measurement of neurotransmitters from extracellular fluid in brain by in vivo microdialysis and chromatography–mass spectrometry». In: *Journal of pharmaceutical and biomedical analysis* 40.3 (2006), pp. 492–499 (cit. on p. 2).

[11] Meleik A Hebert, CRAIG G Van Horne, Barry J Hoffer, and Greg A Gerhardt. «Functional effects of GDNF in normal rat striatum: presynaptic studies using in vivo electrochemistry and microdialysis.» In: *Journal of Pharmacology and Experimental Therapeutics* 279.3 (1996), pp. 1181–1190 (cit. on p. 2).

[12] Peng Song, Neil D. Hershey, Omar S. Mabrouk, Thomas R. Slaney, and Robert T. Kennedy. «Mass Spectrometry "Sensor" for in Vivo Acetylcholine Monitoring». In: *Analytical Chemistry* 84.11 (2012). PMID: 22616788, pp. 4659–4664. DOI: 10.1021/ac301203m. eprint: https://doi.org/10.1021/ac301203m. URL: https://doi.org/10.1021/ac301203m (cit. on p. 2).

[13] Dawei Qi, Qian Zhang, Wanhong Zhou, Jingjing Zhao, Bo Zhang, Yunfei Sha, and Zhiqing Pang. «Quantification of dopamine in brain microdialysates with high-performance liquid chromatography–tandem mass spectrometry». In: *Analytical Sciences* 32.4 (2016), pp. 419–424 (cit. on p. 2).

[14] Alyssa G. Yocky and Dan P. Covey. «Evolution of in vivo dopamine monitoring techniques». In: *Pharmacology Biochemistry and Behavior* 200 (2021), p. 173078. ISSN: 0091-3057. DOI: https://doi.org/10.1016/j.pbb.2020.173078. URL: https://www.sciencedirect.com/science/article/pii/S0091305720306079 (cit. on pp. 2, 3).

[15] Michael D. Nguyen and B. Jill Venton. «Fast-scan Cyclic Voltammetry for the Characterization of Rapid Adenosine Release». In: *Computational and Structural Biotechnology Journal* 13 (2015), pp. 47–54. ISSN: 2001-0370. DOI: https://doi.org/10.1016/j.csbj.2014.12.006. URL: https://www.sciencedirect.com/science/article/pii/S2001037014000567 (cit. on p. 3).

[16] Suelen Lucio Boschen, James Trevathan, Seth A. Hara, Anders Asp, and J. Luis Lujan. «Defining a Path Toward the Use of Fast-Scan Cyclic Voltammetry in Human Studies». In: *Frontiers in Neuroscience* 15 (2021). ISSN: 1662-453X. DOI: 10.3389/fnins.2021.728092. URL: https://www.frontiersin.org/articles/10.3389/fnins.2021.728092 (cit. on p. 3).

[17] Schwerdt H.N. et al. «Long-term dopamine neurochemical monitoring in primates.» In: *Proceedings of the National Academy of Sciences of the United States of America* 114,50 (2017), pp. 13260–13265. DOI: 10.1073/pnas.1713756114 (cit. on p. 3).

[18] Schwerdt H.N. et al. «Cellular-scale probes enable stable chronic subsecond monitoring of dopamine neurochemicals in a rodent model.» In: *Nature Communications Biology* (2018). DOI: 10.1038/s42003-018-0147-y (cit. on p. 3).

[19] Harmain Rafi and Alexander G Zestos. «recent advances in FSCV detection of neurochemicals via waveform and carbon microelectrode modification». In: *Journal of The Electrochemical Society* 168.5 (2021), p. 057520 (cit. on p. 3).

[20] Fangmiao Sun et al. «A genetically encoded fluorescent sensor enables rapid and specific detection of dopamine in flies, fish, and mice». In: *Cell* 174.2 (2018), pp. 481–496 (cit. on pp. 4, 7).

[21] Arnaud Muller, Victory Joseph, Paul A Slesinger, and David Kleinfeld. «Cell-based reporters reveal in vivo dynamics of dopamine and norepinephrine release in murine cortex». In: *Nature methods* 11.12 (2014), pp. 1245–1252 (cit. on pp. 4, 7).

[22] Larry Gold, Nebojsa Janjic, Thale Jarvis, Dan Schneider, Jeffrey J Walker, Sheri K Wilcox, and Dom Zichi. «Aptamers and the RNA world, past and present». In: *Cold Spring Harbor perspectives in biology* 4.3 (2012), a003582 (cit. on p. 4).

[23] Shuaijian Ni et al. «Recent progress in aptamer discoveries and modifications for therapeutic applications». In: *ACS Applied Materials & Interfaces* 13.8 (2020), pp. 9500–9519 (cit. on p. 4).

[24] Chia-Yu Lin, A Balamurugan, Yi-Hsuan Lai, and Kuo-Chuan Ho. «A novel poly (3, 4-ethylenedioxythiophene)/iron phthalocyanine/multi-wall carbon nanotubes nanocomposite with high electrocatalytic activity for nitrite oxidation». In: *Talanta* 82.5 (2010), pp. 1905–1911 (cit. on p. 4).

[25] Chaitali Singhal, John G Bruno, Ankur Kaushal, and Tarun K Sharma. «Recent Advances and a Roadmap to Aptamer-Based Sensors for Bloodstream Infections». In: *ACS Applied Bio Materials* 4.5 (2021), pp. 3962–3984 (cit. on p. 4).

[26] Samy M Shaban and Dong-Hwan Kim. «Recent advances in aptamer sensors». In: *Sensors* 21.3 (2021), p. 979 (cit. on p. 4).

[27] Nako Nakatsuka et al. «Aptamer–field-effect transistors overcome Debye length limitations for small-molecule sensing». In: *Science* 362.6412 (2018), pp. 319–324. DOI: 10.1126/science.aao6750. URL: https://www.science.org/doi/abs/10.1126/science.aao6750 (cit. on pp. 5–7, 9, 25, 51).

[28] Guangfu Wu et al. «Implantable Aptamer-Graphene Microtransistors for Real-Time Monitoring of Neurochemical Release in Vivo». In: *Nano Letters* 22.9 (2022), pp. 3668–3677 (cit. on pp. 5–7, 9).

[29] Nako Nakatsuka, Alix Faillétaz, Dominic Eggemann, Csaba Forró, János Vörös, and Dmitry Momotenko. «Aptamer conformational change enables serotonin biosensing with nanopipettes». In: *Analytical Chemistry* 93.8 (2021), pp. 4033–4041 (cit. on pp. 5, 6, 9–11, 22).

[30] B Jill Venton and Qun Cao. «Fundamentals of fast-scan cyclic voltammetry for dopamine detection». In: *Analyst* 145.4 (2020), pp. 1158–1168 (cit. on p. 7).

[31] Nako Nakatsuka, John M Abendroth, Kyung-Ae Yang, and Anne M Andrews. «Divalent cation dependence enhances dopamine aptamer biosensing». In: *ACS Applied Materials & Interfaces* 13.8 (2021), pp. 9425–9435 (cit. on pp. 7, 25, 51).

[32] Mafalda Abrantes, Diana Rodrigues, Telma Domingues, Siva S Nemala, Patricia Monteiro, Jérôme Borme, Pedro Alpuim, and Luis Jacinto. «Ultrasensitive Dopamine Detection with Graphene Aptasensor Multitransistor Arrays». In: *bioRxiv* (2022) (cit. on p. 7).

[33] Rong Fan, Rohit Karnik, Min Yue, Deyu Li, Arun Majumdar, and Peidong Yang. «DNA translocation in inorganic nanotubes». In: *Nano Letters* 5.9 (2005), pp. 1633–1637 (cit. on p. 8).

[34] Elizabeth A Heins, Zuzanna S Siwy, Lane A Baker, and Charles R Martin. «Detecting single porphyrin molecules in a conically shaped synthetic nanopore». In: *Nano letters* 5.9 (2005), pp. 1824–1829 (cit. on p. 8).

[35] Xiuqing Gong, Amol V Patil, Aleksandar P Ivanov, Qingyuan Kong, Thomas Gibb, Fatma Dogan, Andrew J deMello, and Joshua B Edel. «Label-free in-flow detection of single DNA molecules using glass nanopipettes». In: *Analytical chemistry* 86.1 (2014), pp. 835–841 (cit. on p. 8).

[36] Niya Sa, Wen-Jie Lan, Wenqing Shi, and Lane A Baker. «Rectification of ion current in nanopipettes by external substrates». In: *ACS nano* 7.12 (2013), pp. 11272–11282 (cit. on p. 8).

[37] Zuzanna S Siwy. «Ion-current rectification in nanopores and nanotubes with broken symmetry». In: *Advanced Functional Materials* 16.6 (2006), pp. 735–746 (cit. on p. 8).

[38] Dragoş Constantin and Zuzanna S Siwy. «Poisson-Nernst-Planck model of ion current rectification through a nanofluidic diode». In: *Physical Review E* 76.4 (2007), p. 041202 (cit. on p. 8).

[39] Henry S White and Andreas Bund. «Ion current rectification at nanopores in glass membranes». In: *Langmuir* 24.5 (2008), pp. 2212–2218 (cit. on p. 8).

[40] Mohit Trivedi and Neelkanth Nirmalkar. «Ion transport and current rectification in a charged conical nanopore filled with viscoelastic fluids». In: *Scientific reports* 12.1 (2022), pp. 1–16 (cit. on pp. 8–10).

[41] Shiojenn Tseng, Sheng-Chang Lin, Chih-Yuan Lin, and Jyh-Ping Hsu. «Influences of cone angle and surface charge density on the ion current rectification behavior of a conical nanopore». In: *The Journal of Physical Chemistry C* 120.44 (2016), pp. 25620–25627 (cit. on p. 9).

[42] Javier Cervera, Birgitta Schiedt, Reinhard Neumann, Salvador Mafé, and Patricio Ramırez. «Ionic conduction, rectification, and selectivity in single conical nanopores». In: *The Journal of chemical physics* 124.10 (2006), p. 104706 (cit. on p. 9).

[43] Juan Liu, Maksim Kvetny, Jingyu Feng, Dengchao Wang, Baohua Wu, Warren Brown, and Gangli Wang. «Surface charge density determination of single conical nanopores based on normalized ion current rectification». In: *Langmuir* 28.2 (2012), pp. 1588–1595 (cit. on p. 9).

[44] Ye Ai, Mingkan Zhang, Sang W Joo, Marcos A Cheney, and Shizhi Qian. «Effects of electroosmotic flow on ionic current rectification in conical nanopores». In: *The Journal of Physical Chemistry C* 114.9 (2010), pp. 3883–3890 (cit. on p. 9).

[45] Dong-Huei Lin, Chih-Yuan Lin, Shiojenn Tseng, and Jyh-Ping Hsu. «Influence of electroosmotic flow on the ionic current rectification in a pH-regulated, conical nanopore». In: *Nanoscale* 7.33 (2015), pp. 14023–14031 (cit. on p. 9).

[46] Jyh-Ping Hsu, Shu-Tuan Yang, Chih-Yuan Lin, and Shiojenn Tseng. «Ionic current rectification in a conical nanopore: Influences of electroosmotic flow and type of salt». In: *The Journal of Physical Chemistry C* 121.8 (2017), pp. 4576–4582 (cit. on p. 9).

[47] Chang Wei, Allen J Bard, and Stephen W Feldberg. «Current rectification at quartz nanopipet electrodes». In: *Analytical Chemistry* 69.22 (1997), pp. 4627–4633 (cit. on p. 9).

[48] Ralph MM Smeets, Ulrich F Keyser, Diego Krapf, Meng-Yue Wu, Nynke H Dekker, and Cees Dekker. «Salt dependence of ion transport and DNA translocation through solid-state nanopores». In: *Nano letters* 6.1 (2006), pp. 89–95 (cit. on p. 9).

[49] Zuzanna Siwy, Elizabeth Heins, C Chad Harrell, Punit Kohli, and Charles R Martin. «Conical-nanotube ion-current rectifiers: the role of surface charge». In: *Journal of the American Chemical Society* 126.35 (2004), pp. 10850–10851 (cit. on p. 9).

[50] J Cervera, B Schiedt, and P Ramirez. «A Poisson/Nernst-Planck model for ionic transport through synthetic conical nanopores». In: *EPL (europhysics letters)* 71.1 (2005), p. 35 (cit. on p. 9).

[51] ALIX FAILLETAZ. «APTAMER NANOPIPETTES FOR NEUROCHEMICALQUANTIFICATION IN COMPLEX MEDIA». In: (2021) (cit. on pp. 13, 19, 32, 43).

[52] Marina V Voinova, M Rodahl, M Jonson, and B Kasemo. «Viscoelastic acoustic response of layered polymer films at fluid-solid interfaces: continuum mechanics approach». In: *Physica Scripta* 59.5 (1999), p. 391 (cit. on p. 17).

[53] D Johannsmann, K Mathauer, G Wegner, and W Knoll. «Viscoelastic properties of thin films probed with a quartz-crystal resonator». In: *Physical Review B* 46.12 (1992), p. 7808 (cit. on p. 17).

[54] Arno Domack, Oswald Prucker, Jürgen Rühe, and Diethelm Johannsmann. «Swelling of a polymer brush probed with a quartz crystal resonator». In: *Physical Review E* 56.1 (1997), p. 680 (cit. on p. 17).

[55] John A Nelder. «BJ a Nelder, and R. Mead». In: *A simplex method for function minimization," Comput. J* 7.4 (1965), pp. 308–313 (cit. on p. 17).

[56] Denis Buckingham. «Ultrasensitive and Regenerable Sensing of Dopamine via Aptamer Nanopipettes». In: (2021) (cit. on pp. 19, 31–33, 43).

[57] Tobias Jäggi. «Towards multiplexed sensing using aptamer-modified nanopipettes». In: (2021) (cit. on pp. 32, 43, 54).

[58] A.Stuber et al. «Unpublished». In: () (cit. on pp. 33, 43).

[59] Nada F Atta, Yousef M Ahmed, and Ahmed Galal. «Electrochemical determination of neurotransmitters at crown ether modified carbon nanotube composite: application for sub-nano-sensing of serotonin in human serum». In: *Electroanalysis* 31.7 (2019), pp. 1204–1214 (cit. on p. 32).

[60] Isabel Álvarez-Martos and Elena E Ferapontova. «Electrochemical label-free aptasensor for specific analysis of dopamine in serum in the presence of structurally related neurotransmitters». In: *Analytical chemistry* 88.7 (2016), pp. 3608–3616 (cit. on p. 32).

[61] Mohammad Hasanzadeh, Nasrin Shadjou, and Eskandar Omidinia. «A novel electroanalytical method for simultaneous detection of two neurotransmitter dopamine and serotonin in human serum». In: *Journal of neuroscience methods* 219.1 (2013), pp. 52–60 (cit. on p. 32).

[62] Sarah Egert, Christine Boesch-Saadatmandi, Siegfried Wolffram, Gerald Rimbach, and Manfred J Müller. «Serum lipid and blood pressure responses to quercetin vary in overweight patients by apolipoprotein E genotype». In: *The Journal of nutrition* 140.2 (2010), pp. 278–284 (cit. on p. 32).

[63] Mats Allmyr, Fiona Harden, Leisa-Maree L Toms, Jochen F Mueller, Michael S McLachlan, Margaretha Adolfsson-Erici, and Gunilla Sandborgh-Englund. «The influence of age and gender on triclosan concentrations in Australian human blood serum». In: *Science of the total environment* 393.1 (2008), pp. 162–167 (cit. on p. 32).

[64] James D Neaton and Deborah Wentworth. «Serum cholesterol, blood pressure, cigarette smoking, and death from coronary heart disease overall findings and differences by age for 316099 white men». In: *Archives of internal medicine* 152.1 (1992), pp. 56–64 (cit. on p. 32).

[65] J Yota, J Hander, and AA Saleh. «A comparative study on inductively-coupled plasma high-density plasma, plasma-enhanced, and low pressure chemical vapor deposition silicon nitride films». In: *Journal of Vacuum Science & Technology A: Vacuum, Surfaces, and Films* 18.2 (2000), pp. 372–376 (cit. on p. 39).